CHAPTER 6

High resolution density measurement in some binary liquid crystalline mixtures exhibiting induced smectic A phase

6.1 Introduction

Different types of phase transition in liquid crystals are accompanied by changes in the local molecular ordering and are generally observed by the variation in different anisotropic properties. However, depending on the order of the phase transition it may also be accompanied by the changes in some parameters like enthalpy, density (ρ) *etc*. The variations in density, the associated volume jump and thermal expansion coefficient at the transition have been the subjects of numerous investigations [1–22]. In addition, the pretransitional anomaly in thermal expansion coefficient near the transition temperature is an intriguing topic which can also add an extra dimension to study the critical behavior at the phase transition [19-20].

Experimental determination of several thermodynamic properties of liquid crystals (LCs) provides an idea not only of their fundamental phase behavior, but also of their applications in different fields of science. Density is an important parameter in the study of liquid crystal systems, especially in the investigation of phase transitions [18]. Measurement of density provides clear information regarding the nature of the phase transition and molecular ordering. Further, such studies also endow with a confirmatory experimental evidence for the results obtained by using other well known experimental techniques, such as polarizing

optical microscopy and differential scanning calorimetry that concerns the phase transition temperatures, the nature of the phase transition, and also the thermal stability of different mesophases. The increase in the density values on enhancing the molecular ordering correspond to the increase in molecular attraction. This is perhaps the central driving force for liquid crystal ordering. Hence, it appears very much reasonable to obtain an accurate density data and the coefficient of volume expansion of liquid crystals. Again to understand the fundamental aspect as well as the nature of molecular packing, molecular interactions and usage of LC compounds in different technological applications, density study is very much important. Moreover, precise measurement of density provides a qualitative indication of pretransitional phenomena, strength of the transition and can also offer a unique way to determine the critical exponent at various mesophase transitions for the thermotropic system [19-22]. Although several high resolution experimental techniques have contributed considerably by revealing subtle thermal characteristics of various mesophases in the vicinity of phase transitions [21-22], but a detailed study of high resolution density measurement in binary mixtures of two purely nematogenic compounds showing induced smectic A phase is scanty. Furthermore, density studies by Anton Paar digital density meter in liquid crystals have gained considerable importance in recent time due to its high precision measurement [20-22], even though a large amount of sample (~1.5-2g) is required.

One of the most interesting phenomena reported experimentally for the binary nematic liquid crystal mixtures is the induction of smectic A phase [23-27]. The formation of induced mesophase can arise in binary mesogenic mixtures, showing the more ordered mesophase which is absent in the pure compounds. The induction of new mesophases in binary liquid crystalline mixtures can be caused by the specific interaction between the two different molecules and is related to the formation of molecular complexes. Evidently the interaction between the constituent molecules must be significant in the formation of induced smectic A phase and persuades the nematic phase properties in the neighbourhood of the smectic region of the phase diagram. Many bi-component mixtures comprising of nematic compounds have been observed in which induced smectic A phase was noticed [27-30].

This chapter deals with the phase properties of the binary mixtures of 4-heptyl-4′-*n*-cyanobiphenyl (7CB) and 4-n-pentyl-4′-n′-hexyloxybenzoate (ME6O.5). The results of high resolution density measurement have been presented and the nature of the phase transitions involved across the transformation of different phases has been assessed. Even if the nematic-isotropic (N-I) phase transition has been a subject of active theoretical as well as experimental studies over the last few decades [20-21,31-40], descriptions on the smectic A-isotropic (SmA-I) transition are relatively scarce [41-44]. Therefore, from the density measurements nature of the SmA-I transition has also been studied in detail in the present chapter along with the N-I and smectic A-nematic (SmA-N) phase transitions.

6.2 Materials

The compound 7CB were obtained from Merck (UK) and ME6O.5 from AWAT Co. Ltd. (Poland) and used without further purification. The pure compounds were thoroughly mixed to obtain a homogeneous mixture. The transition temperatures and the structural formulae of the pure compounds are given below:

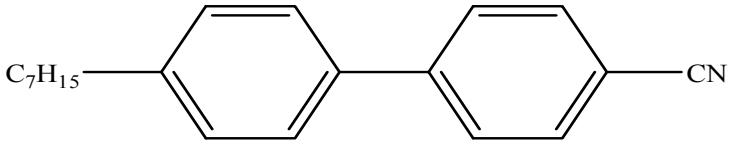

4-heptyl-4′-*n*-cyanobiphenyl (7CB): Cr 30^{o}C N 42.8^{o}C I

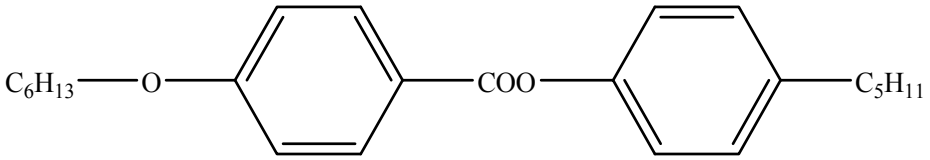

4-n-pentyl-4′-n′-hexyloxybenzoate (ME6O.5): Cr 49.5^{o}C N 62.5^{o}C I

Fourteen mixtures were prepared having mole fraction of 7CB equal to 0.05, 0.095, 0.127, 0.142, 0.164, 0.235, 0.352, 0.424, 0.477, 0.535, 0.600, 0.700 0.800 and 0.852. The phase transition temperatures were determined by a polarizing optical microscope (Motic BA 300) equipped with a Mettler FP900 hot stage.

6.3 Phase diagram

The phase diagram of the binary system 7CB+ME6O.5 has been constructed using the polarizing optical microscopy (POM) by determining the phase transition temperatures of the mixtures made up at specific concentrations. A detailed study of the phase diagram revealed that the transition temperatures are reproducible within ±0.1°C between the heating and cooling cycles for all the studied mixtures. Figure 6.1 illustrates the phase diagram where the nematic–isotropic (N-I), smectic A-isotropic (SmA-I) and smectic A–nematic (SmA-N) transition temperatures are plotted against the mole fraction of 7CB. Even though the two pure compounds used in this study have only the nematic phase but their mixtures show the presence of smectic A (SmA) phase. Of the fourteen mixtures prepared in this study, five shows only the SmA phase while x_{7CB}= 0.852 exhibits only the nematic phase and the rest of the mixtures have both the nematic and smectic A phases. The SmA range shows a domelike structure with a rather strong concentration dependence of the SmA-N transition temperature.

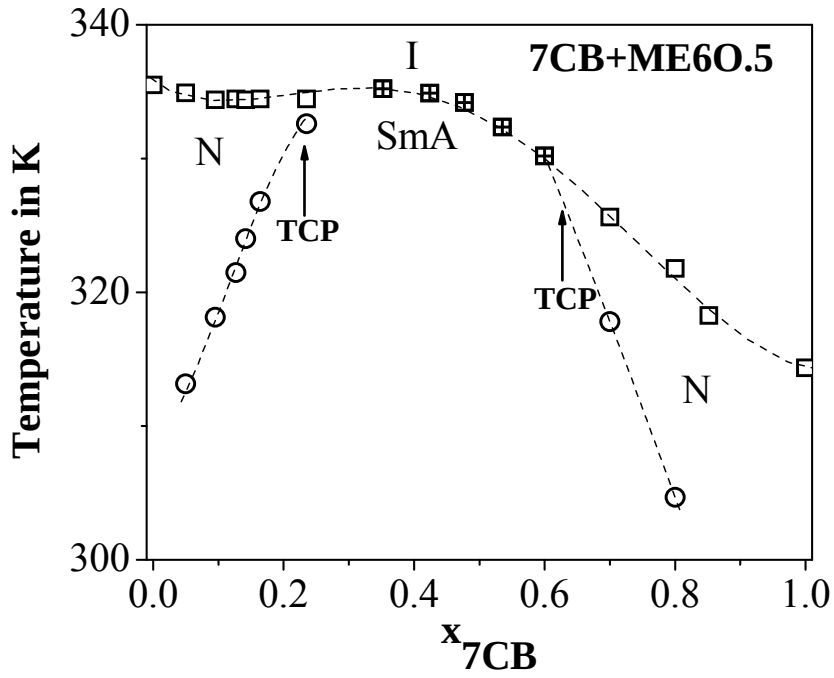

Figure 6.1 Phase diagram of the binary system 7CB+ME6O.5. (□)- nematic-isotropic transition temperature (T_{NI}), (⊞)- smectic A-isotropic transition temperature (T_{SI}), and (o)- smectic A-nematic transition temperature (T_{SN}). TCP indicates the tricritical points.

The nematic range of low mole fraction side decreases with increase in the concentration of 7CB and ceases to exist near $x_{7CB} = 0.352$. For the concentrations $x_{7CB} = 0.352$, 0.424, 0.477, 0.535 and 0.600 the nematic phase disappears and the isotropic phase directly transforms into smectic A phase which is confirmed by the appearance of fan shaped textures (shown in Figure 6.2) [45-46]. Maximum stability of the induced SmA phase is observed near $x_{7CB} = 0.352$. This smectic A-isotropic (SmA-I) transition is a clear manifestation of the concurrent development of the orientational as well as translational ordering which is accompanied by the breaking of infinite rotational symmetry of the completely disordered isotropic phase. Moreover, on the right side of the phase diagram ($x_{7CB} > 0.600$) the width of the nematic phase increases on increasing the concentration of 7CB.

The characteristic textures of different LC phases observed from the polarizing optical microscopy study are presented in Figure 6.2. Schlieren textures and typical marbled type textures have been observed in the nematic phase for the studied mixtures whereas the induced smectic A phase exhibits fan-shaped textures [45-46].

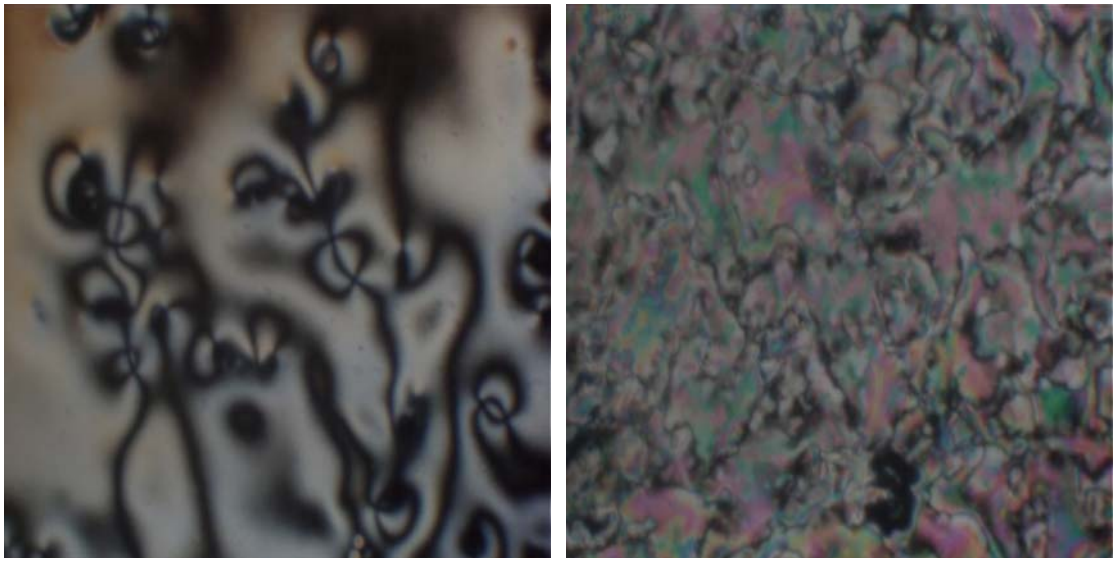

(a) (b)

Figure 6.2 (a-b) Microphotographs (400x magnification) of the textures observed under the polarizing optical microscope for the two mixtures during cooling. (a) Schlieren texture of the nematic phase at 57^{o}C for $x_{7CB} = 0.852$ and (b) Marble type texture of the nematic phase at 58.3^{o}C for $x_{7CB} = 0.127$.

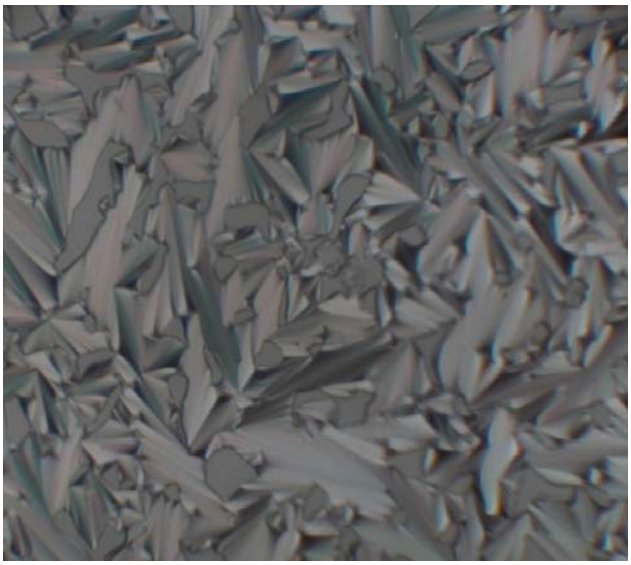

(c)

Figure 6.2(c) Microphotograph of the fan shaped texture observed under the polarizing optical microscope during cooling in the SmA phase at 61.8^{o}C for x_{7CB} = 0.424.

6.4 Density measurements

The results of density measurements for different mixtures in the isotropic, nematic and smectic A phases are presented in Figure 6.3(a-l). The density value increases almost linearly with decrease in temperature in different phases, except across the phase transformations. Near the phase transition region a non-linear behavior of temperature dependent density has been observed, indicating a strong pretransitional change on approaching the transition. At the N-I phase transition the density values exhibit a sudden change before it attains the equilibrium value of the next lower temperature phase, thus indicating an alteration in the molecular ordering from the disordered isotropic phase to ordered nematic phase. Moreover, the slope of the density data increases on entering the nematic phase from the isotropic phase, which indicates the relatively closer packing of the orientationaly ordered molecules in the nematic phase. Note that the density change at the N-I phase transition for all the studied mixtures is well defined and corresponds to a change in the density ($\Delta\rho/\rho$) value ranging between 1.9×10^{-3} to 2.9×10^{-3} g/cm^3. This is very much reliable with the thermodynamic description of the weakly first order phase transition [47-50].

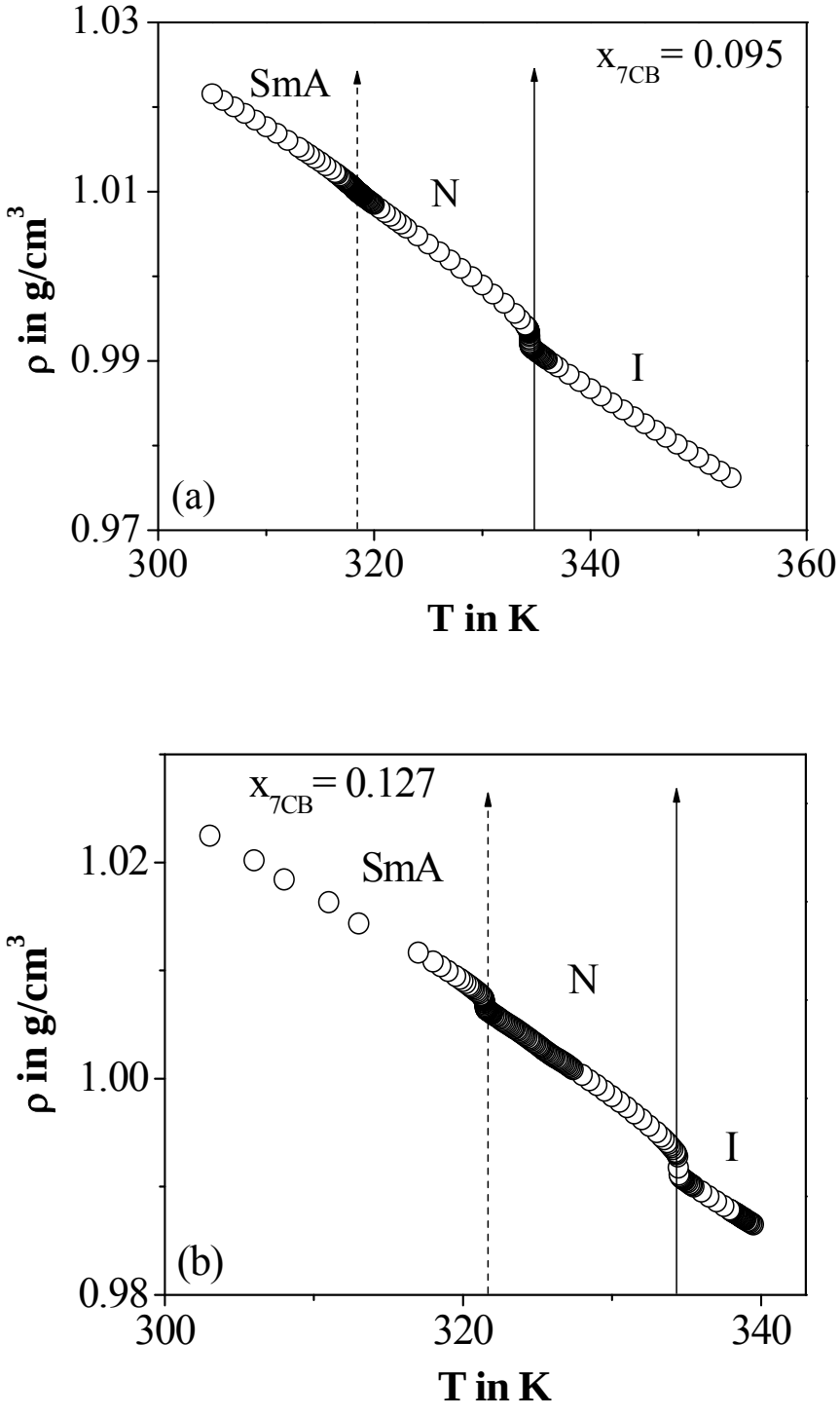

Figure 6.3(a-b) Temperature dependence of density for (a) x_{7CB} = 0.095 and (b) x_{7CB} = 0.127 in the isotropic, nematic and smectic A phases. Solid arrow and dashed arrow denote the nematic-isotropic (N-I) and smectic A-nematic (SmA-N) transition temperatures respectively.

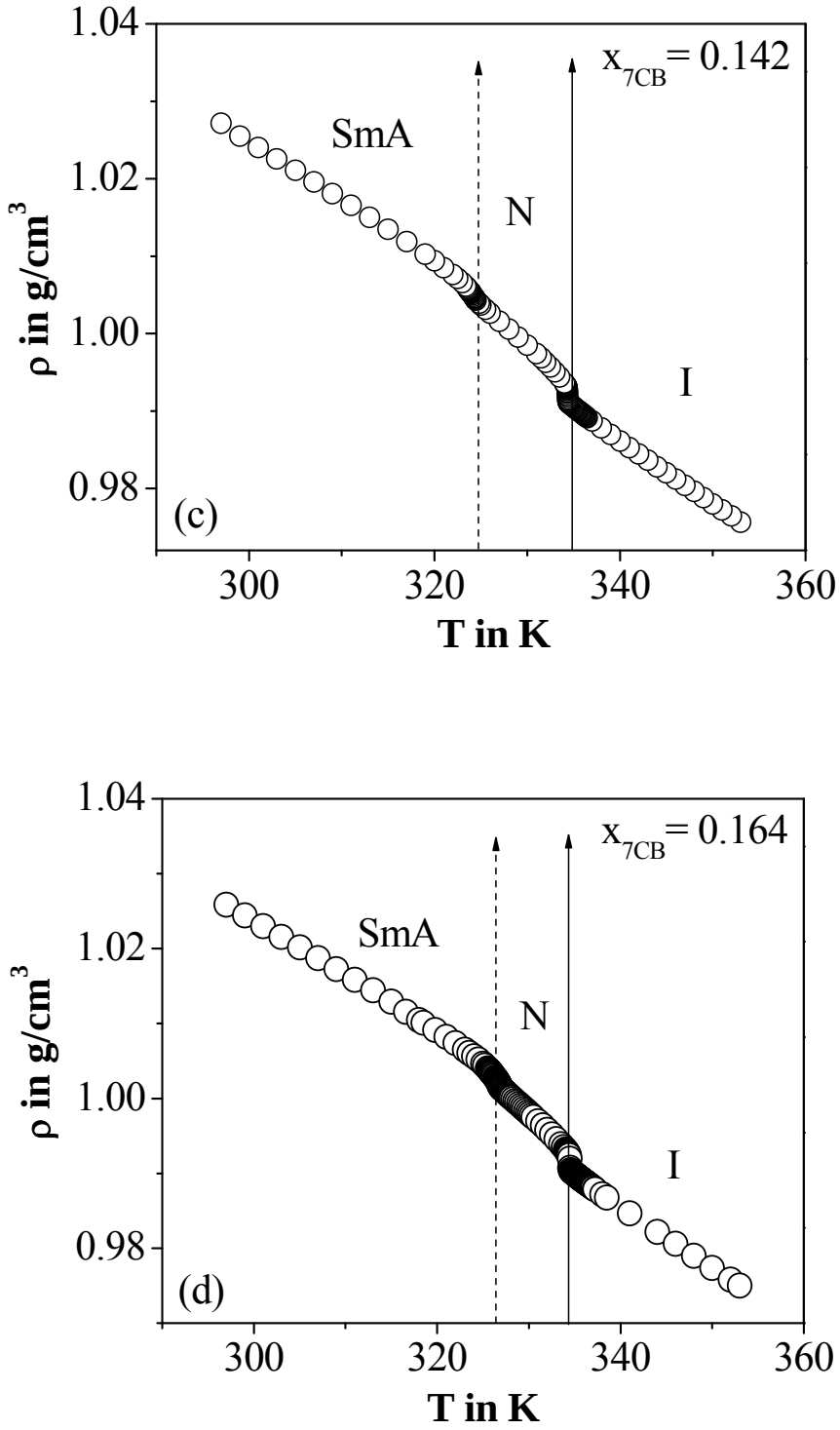

Figure 6.3(c-d) Temperature dependence of density for (c) x_{7CB} = 0.142 and (d) x_{7CB} = 0.164 in the isotropic, nematic and smectic A phases. Solid arrow and dashed arrow denote the nematic-isotropic (N-I) and smectic A-nematic (SmA-N) transition temperatures respectively.

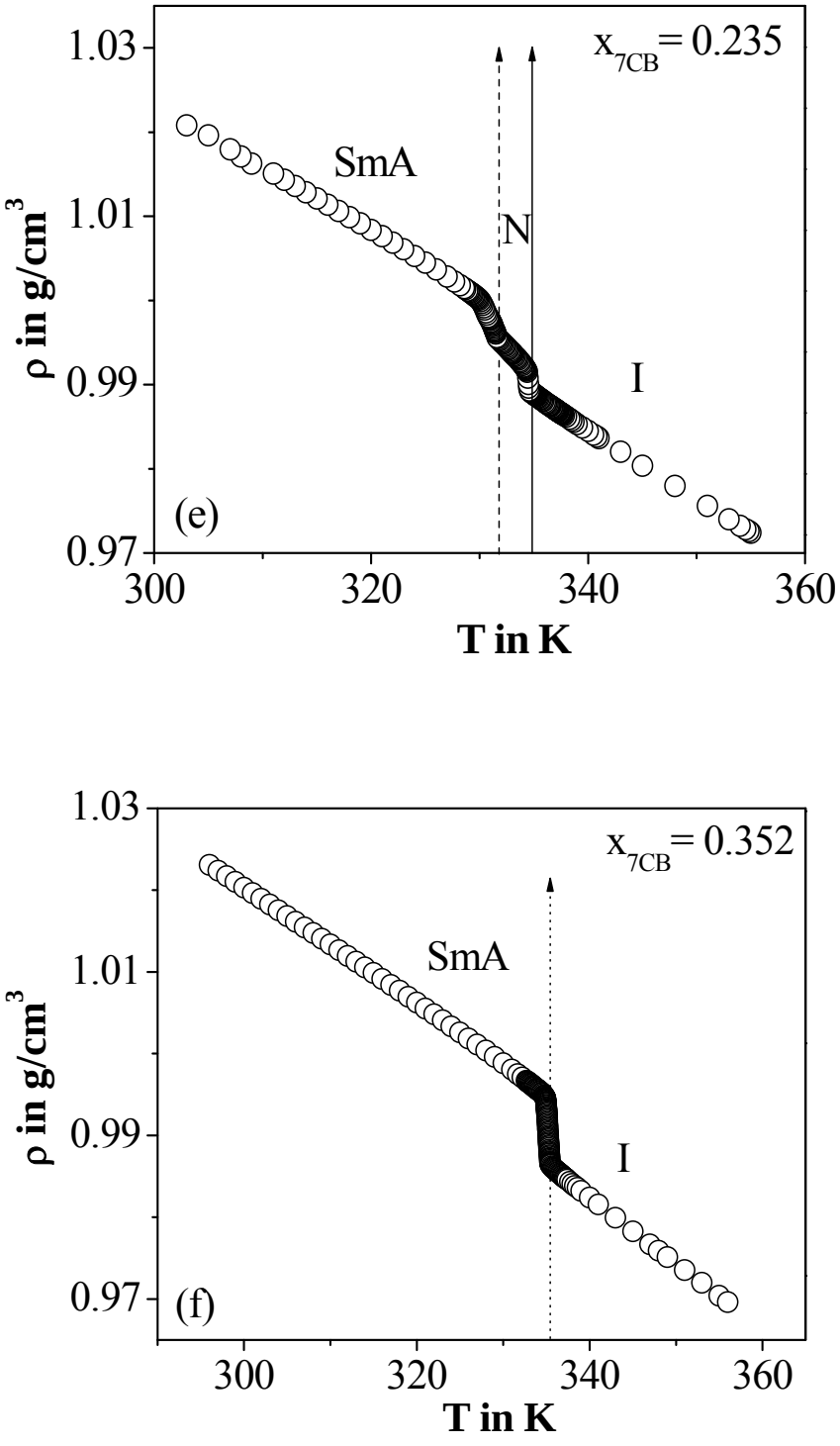

Figure 6.3(e-f) Temperature dependence of density for (e) x_{7CB} = 0.235 and (f) x_{7CB} = 0.352 in the isotropic, nematic and smectic A phases. Solid arrow, dashed arrow and dotted arrow (for x_{7CB} = 0.352) denote the nematic-isotropic (N-I), smectic A-nematic (SmA-N) and smectic A-isotropic (SmA-I) transition temperatures respectively.

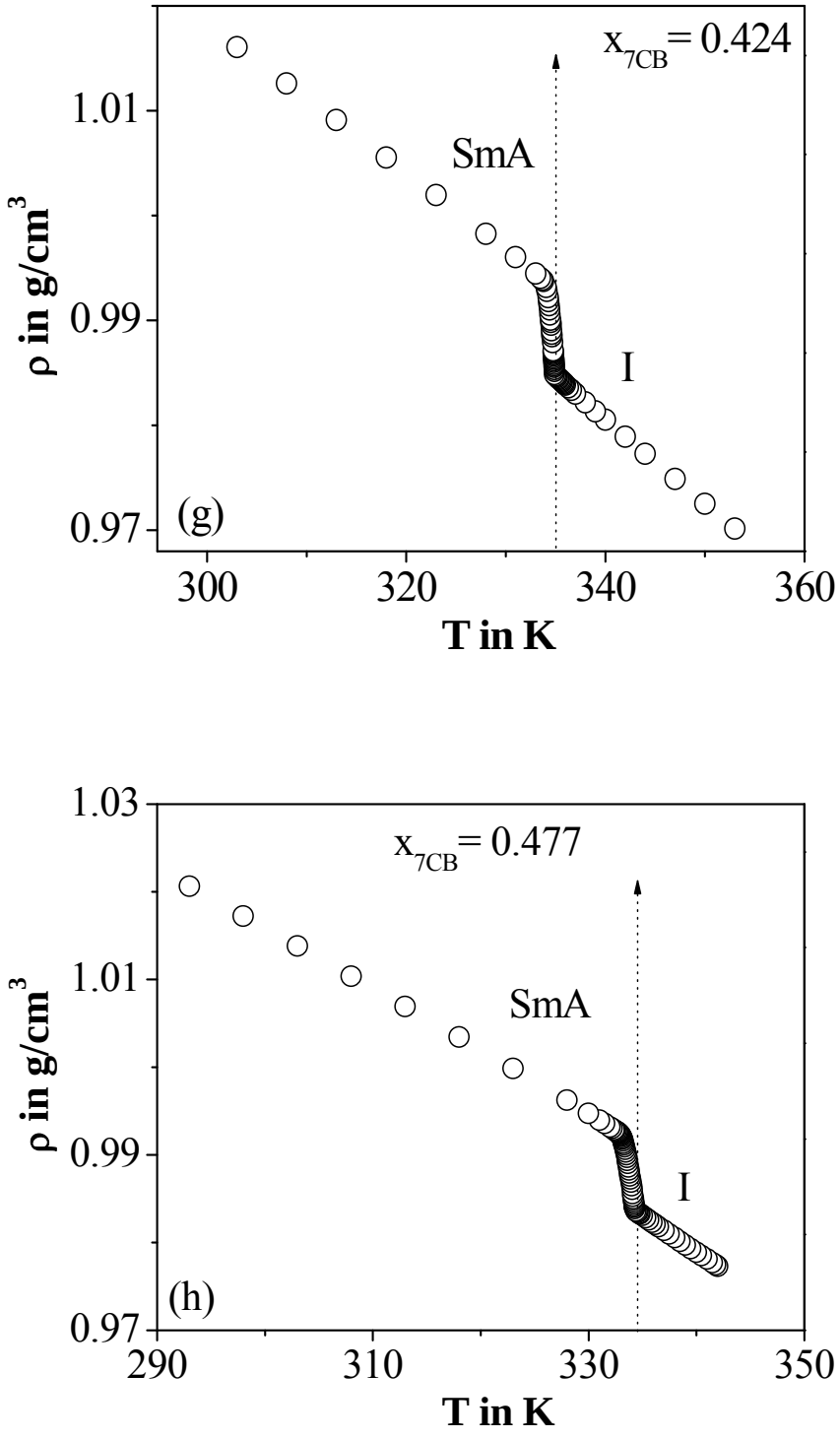

Figure 6.3(g-h) Temperature dependence of density for (g) x_{7CB} = 0.424 and (h) x_{7CB} = 0.477 in the isotropic and smectic A phases. Dotted arrow denotes the smectic A-isotropic (SmA-I) transition temperature.

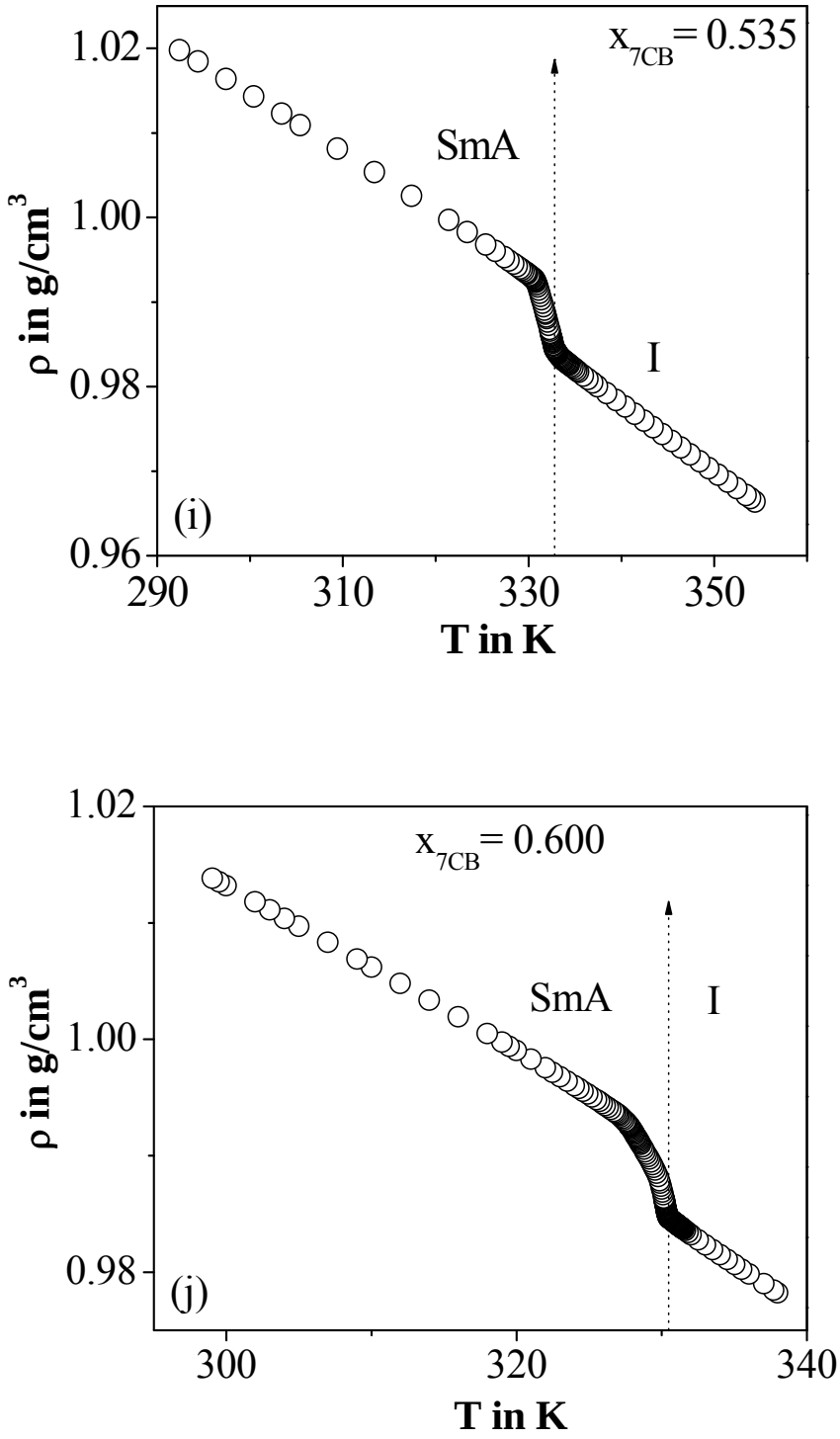

Figure 6.3 (i-j) Temperature dependence of density for (i) x_{7CB} = 0.535 and (j) x_{7CB} = 0.600 in the isotropic and smectic A phases. Dotted arrow denotes the smectic A-isotropic (SmA-I) transition temperature.

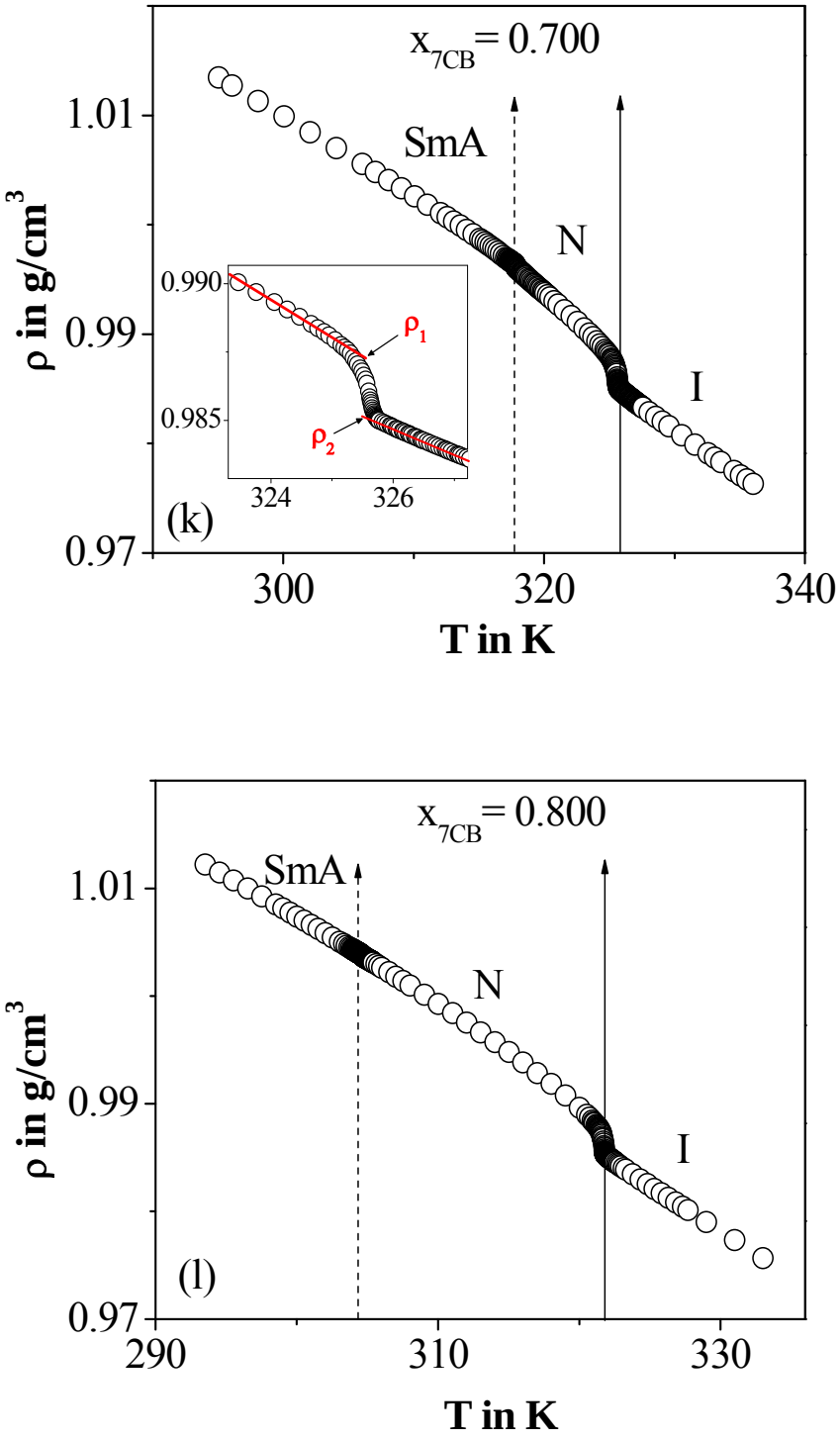

Figure 6.3(k-l) Temperature dependence of density for (k) x_{7CB} = 0.700 and (l) x_{7CB} = 0.800 in the isotropic, nematic and smectic A phases. Solid arrow and dashed arrow denote the nematic-isotropic (N-I) and smectic A-nematic (SmA-N) transition temperatures respectively. In the inset variation of ρ near T_{NI} is shown. ρ_1 and ρ_2 are density values obtained by extrapolation on either side of T_{NI}.

The density jump, ($\Delta\rho/\rho$), is calculated as the vertical distance between the density values (ρ_1 and ρ_2 as shown in the inset of Figure 6.3 (k)) obtained by linear extrapolation from either sides of the transition, *i.e.* $[\{(\rho_1-\rho_2)\}/\{½(\rho_1+\rho_2)\}]$. The calculated $\Delta\rho/\rho$ values suggest that the N-I transition to be a weakly first order phase transition. This is very much comparable to the value reported by the different researchers for diverse LC compounds [18, 47-50]. As far as the smectic A-isotropic (SmA-I) transition is concerned, it is accompanied by a large density jump of 7.2×10^{-3} to 9.7×10^{-3} g/cm^3 compared to the N-I transition. Moreover, for the concentrations x_{7CB} = 0.095, 0.127, 0.142, 0.164, 0.235, 0.700 and 0.800 within the experimental resolution, there is no sharp discontinuity in the density values near the SmA-N transition temperature (T_{SN}). Even though the density changes smoothly at T_{SN}, there is an overall increase in its value in going from the smectic A to nematic phase. The temperature dependence of ρ is fairly linear on both the nematic and smectic A sides, except in the immediate vicinity of the SmA-N transition where it demonstrates a pretransitional behavior. The ρ *vs* T curve also reveals that the pretransitional effect near the SmA-N transition is much weaker than the same at the N-I or SmA-I transition. The $\Delta\rho/\rho$ value at the SmA-N transition varies from 8.2×10^{-5} to 2.7×10^{-3} g/cm^3 for different mixtures.

The first-order phase transition is generally characterized by a discontinuity or a steep change in the specific volume associated with a thermal expansion coefficient $(-1/\rho)(d\rho/dT)$. Furthermore, the thermal expansion coefficient derived from the density data points provides information about the nature of SmA-N, N-I or SmA-I transitions because it shows the same critical behavior as revealed by the specific heat capacity data (C_P) at the transition. There are several reports in the literature which show that analysis of the thermal expansion coefficient yields critical exponents characterizing the critical behavior at the transition in excellent agreement with those obtained from the specific heat capacity studies [19-21,51-52]. Indeed, this resemblance was first demonstrated by Pippard [53] and afterward by Garland [54] along the lambda (λ) transition. Therefore, it certainly reflects that the two independently obtained experimental data can be represented by a same power law expression with same critical exponent but different critical amplitudes.

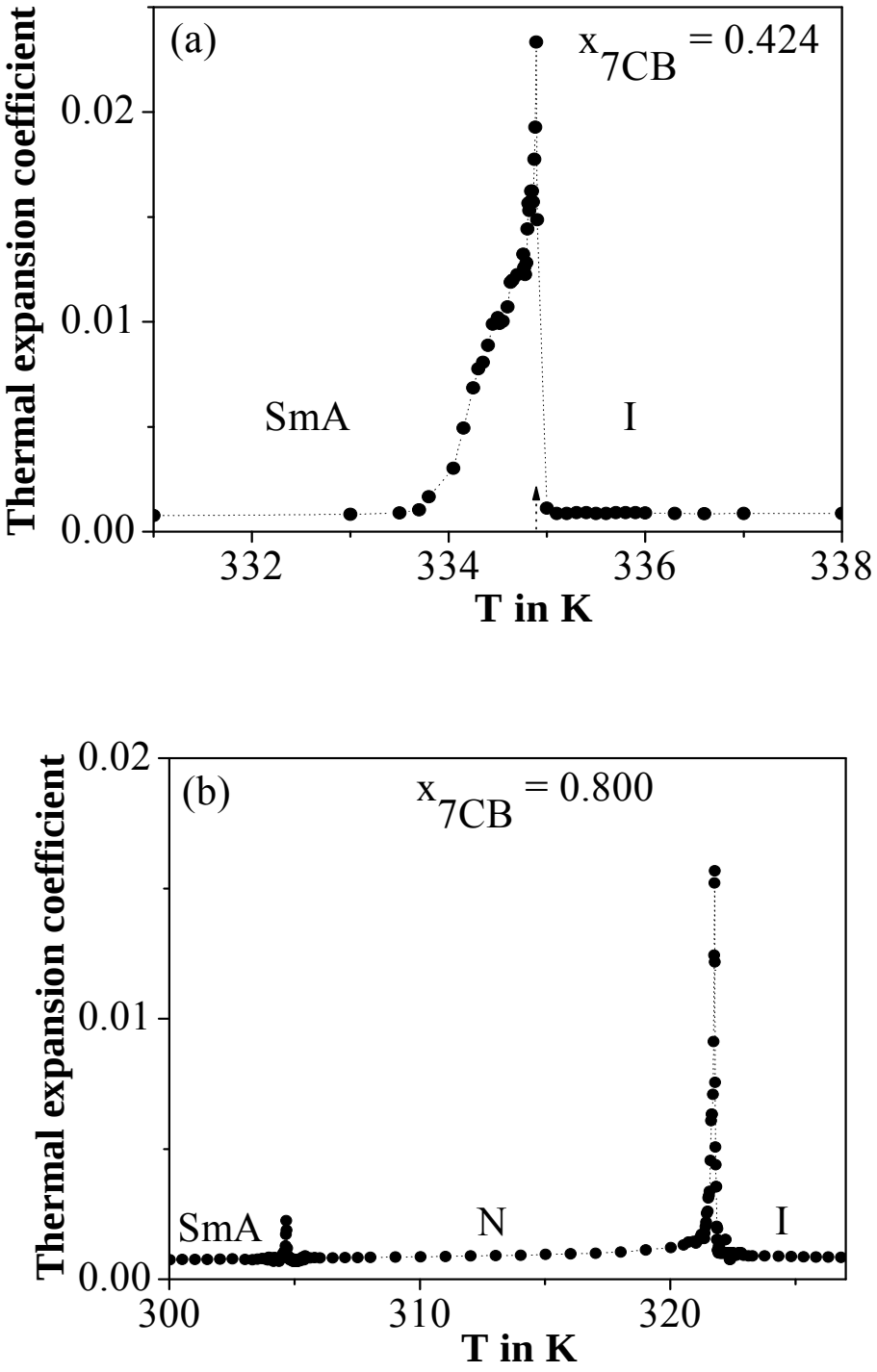

Figure 6.4(a-b) Thermal expansion coefficient for (a) x_{7CB} = 0.424 near the smectic A-isotropic (SmA-I) transition, (b) x_{7CB} = 0.800 near the nematic-isotropic (N-I) and smectic A-nematic (SmA-N) transitions. Results have been calculated from the pairs of neighbouring density data points.

Figure 6.4(a-b) depicts the change in the thermal expansion coefficient at the SmA-I, N-I and SmA-N transitions for the two representative concentrations. Note that the thermal expansion coefficient at both the N-I and SmA-I phase transitions changes much faster than the same at the SmA-N transition. The temperature dependences of thermal expansion coefficient exhibit obvious critical behavior near the transitions. But the calculated data show some scattered values innate to the derivative procedure of the density, which might create a certain difficulty in the rigorous fitting of the data. This difficulty can be prevailed over if one avoid the numerical derivative part and use the molar volume data (V_T). The molar volume is an important parameter that can be measured with high degree of accuracy directly from the experimentally obtained density values with the help of molecular weight and is very effective like other thermodynamic parameters that are capable of producing singularities at the phase transitions. Moreover, to complete the thermodynamic description of a phase V_T is an essential parameter. In this case the data analysis has been performed by considering the logarithm of the molar volume ($\ln V_T$) instead of the thermal expansion coefficient. Figure 6.5(a-l) illustrates the logarithm of molar volume as a function of temperature in the vicinity of N-I and SmA-I phase transitions for the investigated concentrations. An attempt has been made to quantify the critical behavior of $\ln V_T$ associated with the N-I and SmA-I transitions by using the following fitting equations [20-21]

$$\ln V_T = E_0^I + E_1^I(T - T^*) + E_2^I(T - T^*)^2 + A^I(T - T^*)^{1-\alpha} \qquad (6.1)$$

$$\text{for } T > T_{NI} = T^* + \Delta T^*$$

$$\ln V_T = E_0^N + E_1^N(T - T^{**}) + E_2^N(T - T^{**})^2 + A^N(T - T^{**})^{1-\alpha} \qquad (6.2)$$

$$\text{for } T < T_{NI} = T^{**} - \Delta T^{**}$$

where T* represents the temperature at which the N-I transition would occur coming from the isotropic phase if it was second-order and T** has the same meaning when temperature increases from the nematic phase. These critical temperatures T* and T** are often called the spinodal temperatures which belong to the spinodal curve having a maximum at the critical point [19]. α is the specific heat critical exponent which should presume a value 0.5 according to the tricritical hypothesis [55]. $E_0^I, E_0^N, E_1^I, E_1^N, E_2^I, E_2^N, A^I, A^N$ are the independent coefficients

having different values in two phases. The superscripts 'I' and 'N' in the relevent coeffecients represent the value of the parameter in the isotropic and nematic phases respectively. Therefore, in case of the SmA-I transition the superscript 'N' has been replaced by 'S'. The transition temperature T_{NI} has also been changed to T_{SI} in Equation (6.1) and (6.2) accordingly.

Fitting has been performed by considering all the coefficients as a free parameter. Inclusion of this fact improves the fitting quality as it has been seen that (in Figure 6.5) the fitted curve so obtained describes $\ln V_T$ data very well for all the studied concentrations of the present binary system. In addition, the quality of all fits has been tested by calculating the reduced χ^2 [56]. For a correct error estimation and a quality of fit corresponding to the experimental error, the χ^2 value should close to unity. In this case χ^2 ranging from 1.21 to 1.47 indicating a good fit to the data points.

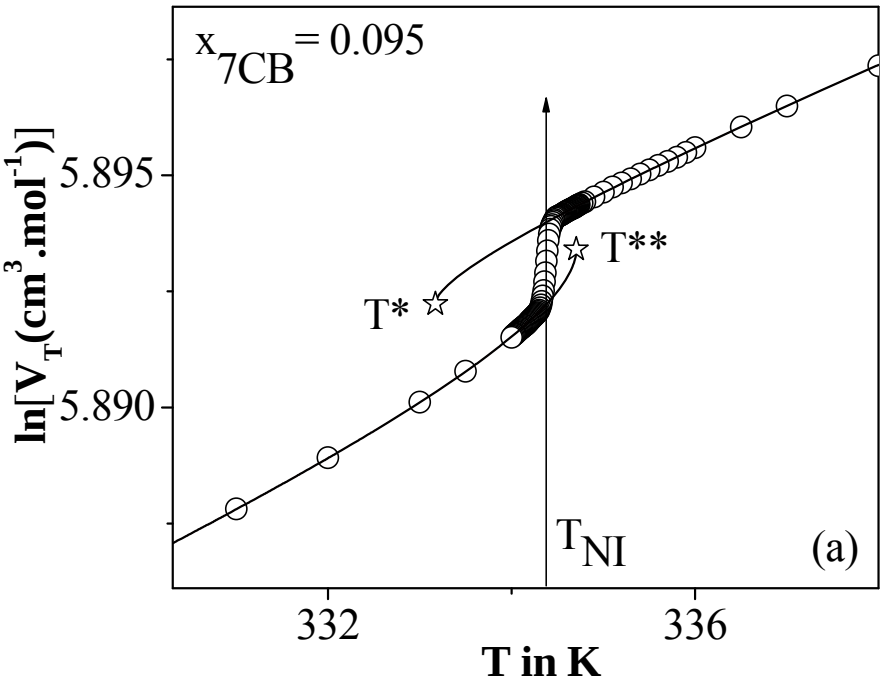

Figure 6.5(a) Logarithm of molar volume as a function of temperature for x_{7CB} = 0.095 in the vicinity of nematic-isotropic (N-I) phase transition. Solid lines represent the fit according to Equation (6.1) and (6.2). The temperatures T* and T** are indicated with a star symbol (☆). Vertical arrow denotes the N-I transition temperature (T_{NI}).

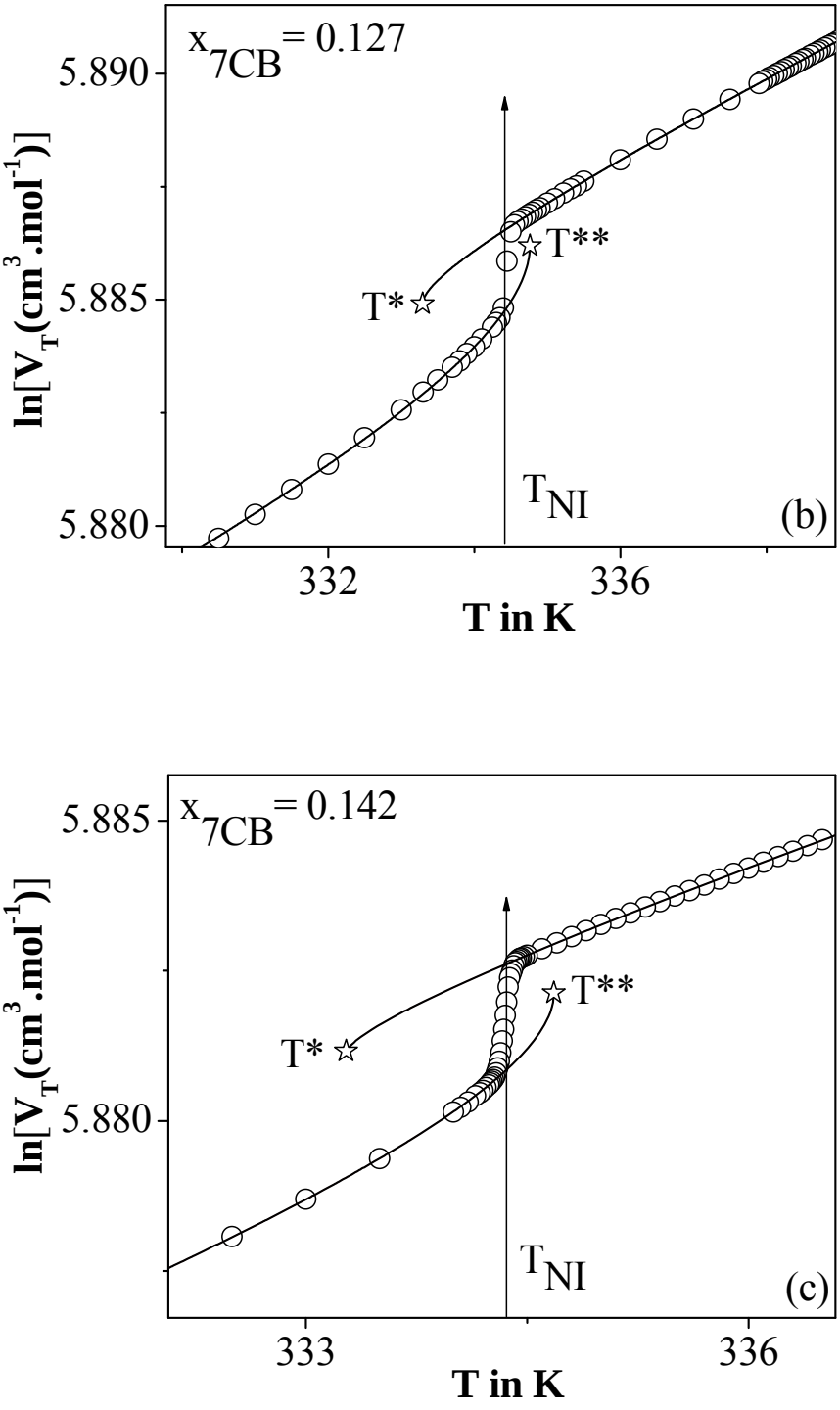

Figure 6.5(b-c) Logarithm of molar volume as a function of temperature for (b) x_{7CB} = 0. 127 and (c) x_{7CB} = 0.142 in the vicinity of nematic-isotropic (N-I) phase transition. Solid lines represent the fit according to Equation (6.1) and (6.2). The temperatures T* and T** are indicated with a star symbol (☆). Vertical arrow denotes the N-I transition temperature (T_{NI}).

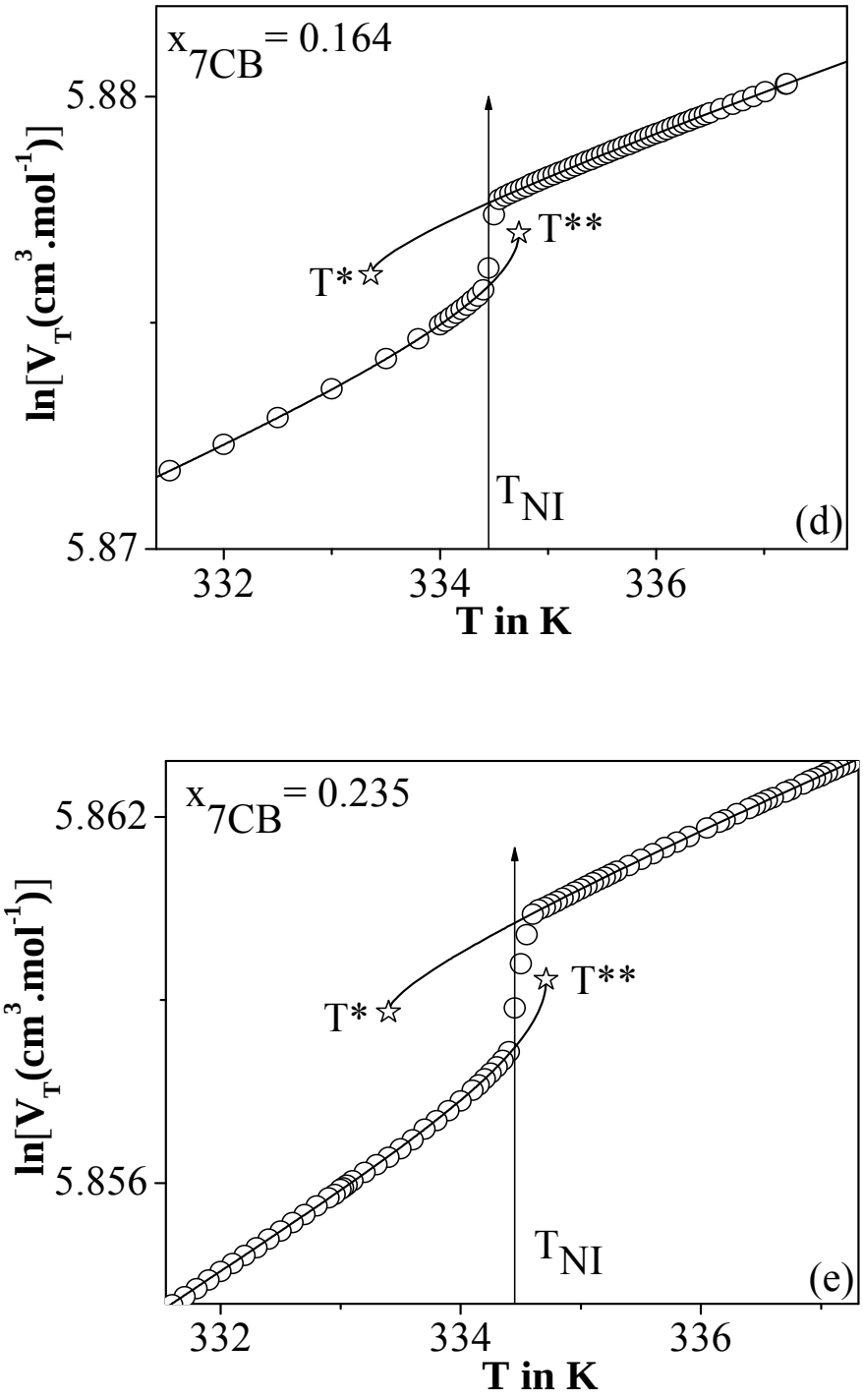

Figure 6.5(d-e) Logarithm of molar volume as a function of temperature for (d) x_{7CB} = 0.164 and (e) x_{7CB} = 0.235 in the vicinity of nematic-isotropic (N-I) transition. Solid lines represent the fit according to Equation (6.1) and (6.2). The temperatures T* and T** are indicated with a star symbol (☆). Vertical arrow denotes the N-I transition temperature (T_{NI}).

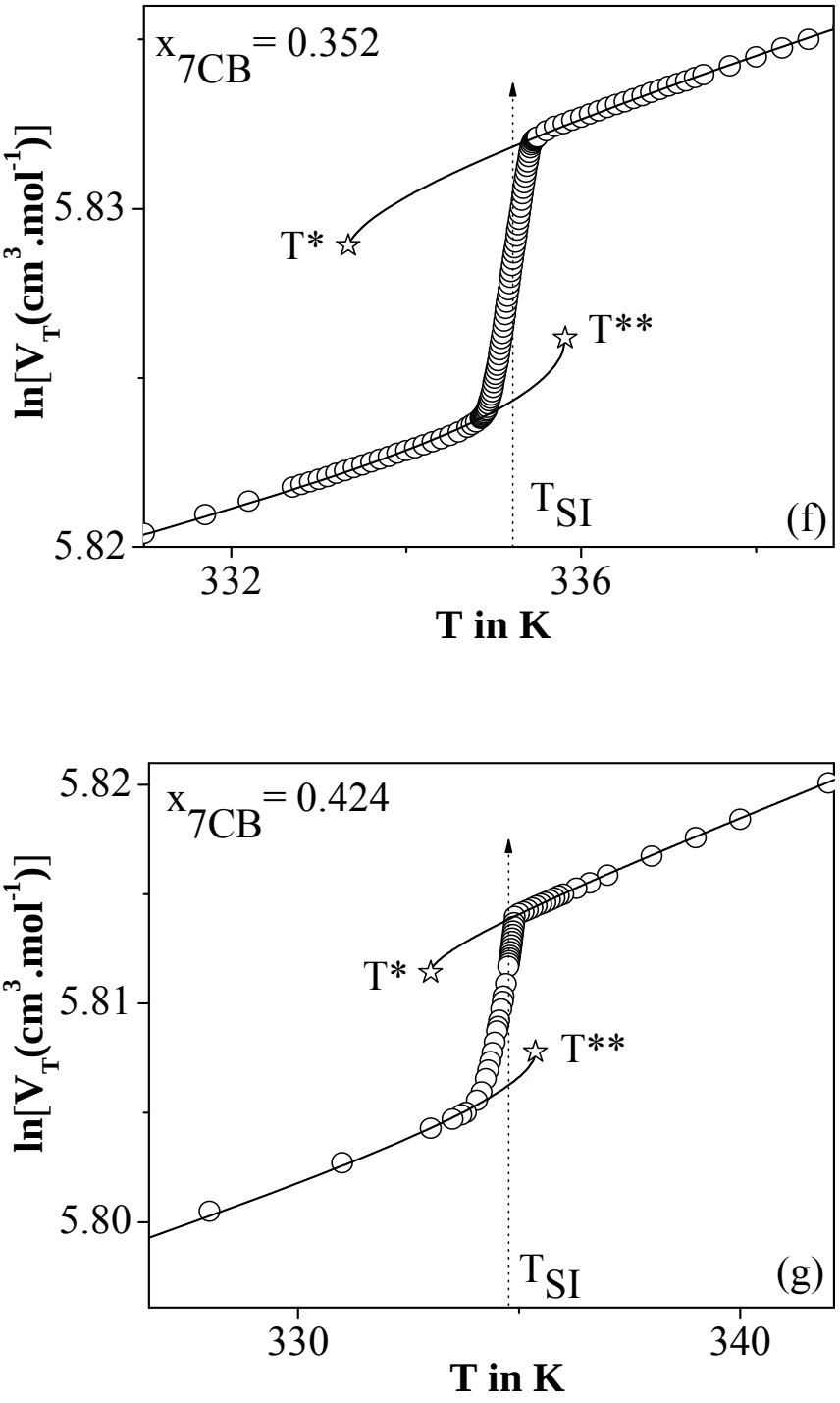

Figure 6.5(f-g) Logarithm of molar volume as a function of temperature for (f) x_{7CB} = 0.352 and (g) x_{7CB} = 0.424 in the vicinity SmA-I transition. Solid lines represent the fit according to Equation (6.1) and (6.2). The temperatures T* and T** are indicated with a star symbol (☆). Dotted arrow denotes the SmA-I transition temperature (T_{SI}).

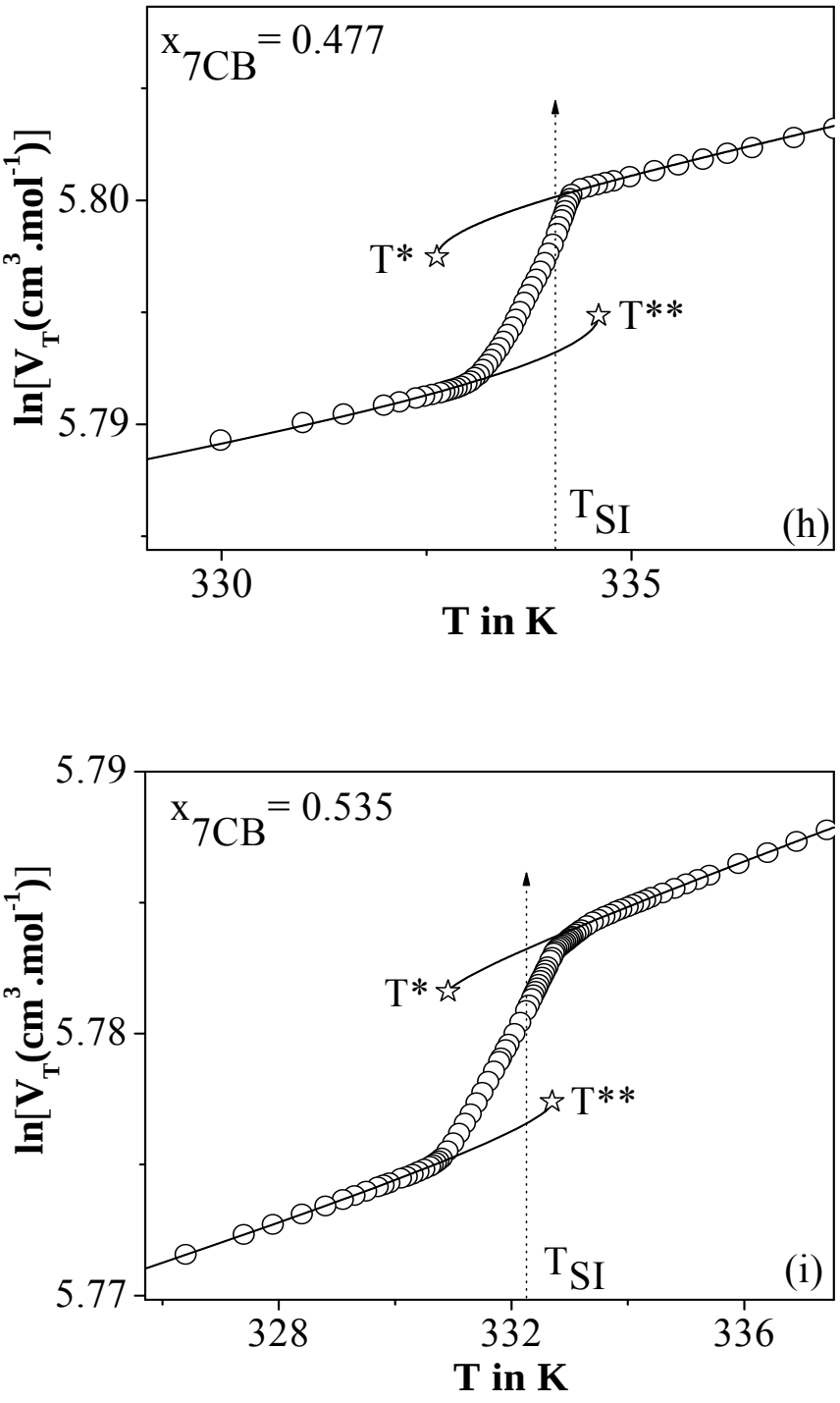

Figure 6.5(h-i) Logarithm of molar volume as a function of temperature for (h) x_{7CB} = 0.477 and (i) x_{7CB} = 0.535 in the vicinity of smectic A-isotropic (SmA-I) transition. Solid lines represent the fit according to Equation (6.1) and (6.2). The temperatures T* and T** are indicated with a star symbol (☆). Dotted arrow denotes the SmA-I transition temperature (T_{SI}).

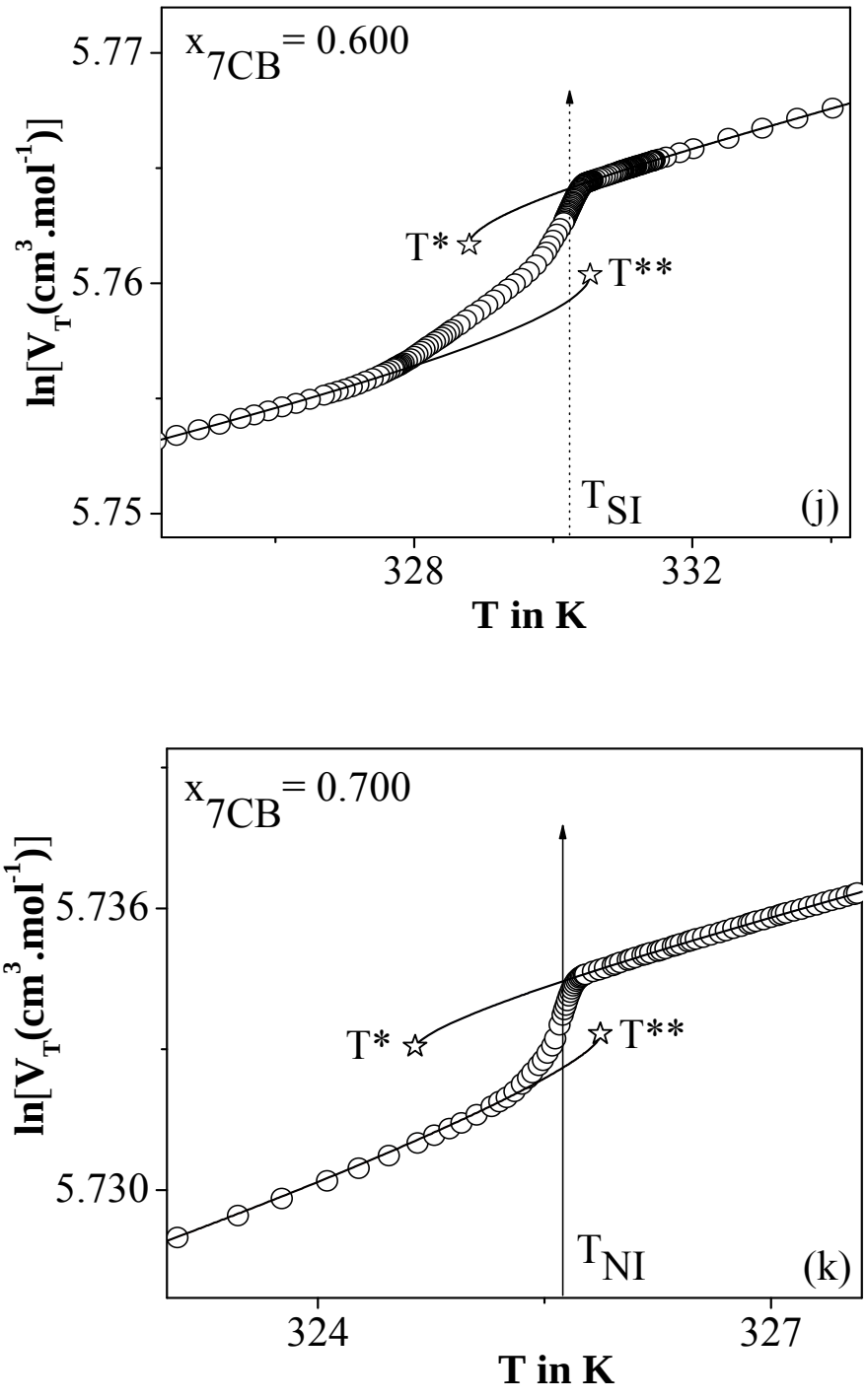

Figure 6.5(j-k) Logarithm of molar volume as a function of temperature for (j) x_{7CB} = 0.600 and (k) x_{7CB} = 0.700 in the vicinity of SmA-I and N-I transitions respectively. Solid lines represent the fit according to Equation (6.1) and (6.2). The temperatures T* and T** are indicated with a star symbol (☆). Solid and dotted arrows denote the N-I transition and SmA-I transition temperatures respectively.

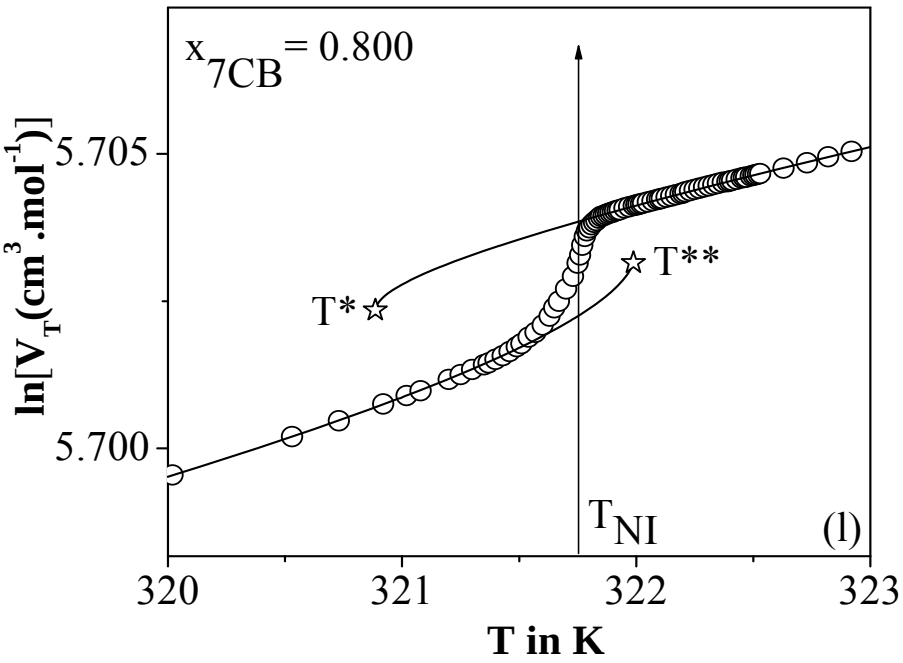

Figure 6.5(l) Logarithm of molar volume as a function of temperature for x_{7CB} = 0.800 in the vicinity of nematic-isotropic (N-I) transition. Solid lines represent the fit according to Equation (6.1) and (6.2). The temperatures T* and T** are indicated with a star symbol (☆). Vertical arrow denotes the N-I transition temperature (T_{NI}).

Generally, the spinodal temperature for the isotropic phase *i.e.* T* is determined by a linear extrapolation method from diverse experimental techniques such as scattered light intensity measurements [57], Cotton-Mouton effect [58], Kerr effect [59-60], dielectric permittivity measurements [38,61-62] or by fitting the dielectric permittivity as a function of temperature [38,62-68]. On the other hand the spinodal temperature of the nematic phase *i.e.* T** can be found from the temperature variation of the dielectric strength [65], birefringence [69-70] or average dielectric permittivity [63,67-68]. But it is very hard to determine T** from the above mentioned parameters because sometimes it results a value even less than the nematic-isotropic phase transition temperature (T_{NI}) [63]. In the present case, the thermodynamic values of the spinodal temperatures have been determined by a fitting procedure through the temperature dependence of molar volume (V_T) data measured in the vicinity of the N-I or SmA-I phase transitions. The fitting results of the $\ln V_T$ values in both sides of the studied transitions,

according to Equations (6.1) and (6.2) are consigned in Table 6.1. Furthermore, the fitted curves are extrapolated to the spinodal temperatures T* and T** as shown in Figure 6.5. These spinodal temperatures (T* and T**) along with the transition temperatures (T_{NI} or T_{SI}) allow one to find out both the discontinuity ΔT* and ΔT** as well as (T**–T*) as tabulated in the Table 6.1. The temperature difference T**–T* can be stated as the width of the metastable state for the studied phase transitions. Interestingly, the parameter ΔT* *i.e*. the lower stability temperature of the super cooled isotropic phase contains information on how far a weakly first order phase transition is from a truly second order phase transition. The fitting results ΔT* values lies in the range 0.88K to 1.05K and 1.4K to 1.9K while ΔT** is ranging between 0.23K to 0.33K and 0.34K to 0.6K for the N-I and SmA-I transitions respectively. It is obvious from the above results that the value of the temperature difference T_{SI} – T* or T**– T_{SI} is higher than that of T_{NI} – T* or T**– T_{NI}. Therefore, the neighborhood of a SmA-I phase transition has a striking influence on the pretransitional behavior in the isotropic phase. Moreover, the width of the metastable region varies from 1.11K to 1.53K for the N-I transition whereas for the SmA-I transition it varies from 1.74K to 2.5K. It should be stressed that the width of the metastable region for the N-I transition is less than that extracted for the SmA-I transition, since this is anticipated for a comparatively weaker first order phase transition of a nearly tricritical character. Another important observation is that as the concentration of the polar compound 7CB increases the discontinuity ΔT* as well as ΔT** at the transition decreases for both the N-I and SmA-I transitions. Besides, the ratio of the two discontinuities (ΔT*/ΔT**) is supposed to be non-universal and varying from 3.16 to 4.15 which significantly differs from the theoretical Landau-de Gennes value of 8 [19].

According to Mukherjee [41], presence of a cubic coefficient in the free energy density expansion in terms of the order parameter confirms the first order nature of SmA-I transition. Also the SmA-I transition is accompanied by a jump of the order parameter at T_{SI}. Ocko *et al.* [71] have reported that the smectogenic LC 4-*n*-dodecyl-4′-cyanobiphenyl (12CB) undergoes a first order SmA-I transition. From the birefringence study Olbrich *et al.* [72] argued that both the nematic and smectic fluctuations become significant near the SmA-I transition temperature.

Table 6.1 Results of fit to Equation (6.1) and (6.2) in the isotropic and nematic or smectic A phase for the different mixtures

Mole fraction x_{5DBT}		E_0^I or E_0^N	E_1^I or E_1^N	E_2^I or E_2^N	A^I or A^N	ΔT* or ΔT**	α	χ^2
0.095	$T>T_{NI}$	5.892±0.001	6.6E-4±1E-5	1.35E-6±1E-7	8.7E-4±2E-5	1.21	0.499±0.008	1.37
	$T<T_{NI}$	5.893±0.003	-5.8E-4±E-5	–3.71E-6±1E-7	–0.001±5E-5	0.33	0.494±0.004	
0.127	$T>T_{NI}$	5.88±0.002	6.6E-4±1E-5	2.00E-6±2E-7	8.3E-4±1E-5	1.16	0.499±0.007	1.25
	$T<T_{NI}$	5.88±0.001	–3.6E-4±1E-5	–10.0E-6±1E-7	–0.002±1E-5	0.31	0.494±0.009	
0.142	$T>T_{NI}$	5.88±0.001	7E-4±2E-5	5.53E-6±1E-7	7.3E-4±1E-5	1.12	0.500±0.001	1.29
	$T<T_{NI}$	5.88±0.001	–5E-4±1E-5	–10.0E-6±5E-7	–0.002±2E-5	0.30	0.497±0.002	
0.164	$T>T_{NI}$	5.87±0.003	6.8E-4±1E-5	1.04E-6±1E-7	8.1E-4±2E-5	1.09	0.505±0.008	1.33
	$T<T_{NI}$	5.87±0.002	–5.1E-4±1E-5	–20.0E-6±3E-7	–0.002±3E-5	0.28	0.499±0.002	
0.235	$T>T_{NI}$	5.85±0.003	7.2E-4±2E-5	5.03E-7±6E-8	6.9E-4±1E-5	1.05	0.506±0.004	1.28
	$T<T_{NI}$	5.85±0.001	–5.4E-4±1E-5	–40.0E-6±1E-7	–0.001±7E-5	0.26	0.509±0.008	
0.352	$T>T_{SI}$	5.82±0.011	5E-4±1E-5	3.50E-6±2E-7	0.001±6E-5	1.90	0.501±0.005	1.34
	$T<T_{SI}$	5.82±0.007	–7E-4±2E-5	–20.0E-6±1E-7	–0.002±4E-5	0.60	0.499±0.004	

Table 6.1 (Continued) Results of fit to Equation (6.1) and (6.2) in the isotropic and nematic or smectic A phase for the different mixtures

Mole fraction x_{5DBT}		E_0^I or E_0^N	E_1^I or E_1^N	E_2^I or E_2^N	A^I or A^N	ΔT^* or ΔT^{**}	α	χ^2
0.424	$T>T_{SI}$	5.811±0.002	6.0E-4±2E-5	2.94E-6±1E-7	0.001±2E-5	1.89	0.503±0.002	1.21
	$T<T_{SI}$	5.807±0.001	–3.8E-4±1E-5	–3.10E-6±1E-7	–0.001±3E-5	0.48	0.499±0.007	
0.477	$T>T_{SI}$	5.797±0.006	2.5E-4±1E-5	20.0E-6±1E-7	0.002±6E-5	1.56	0.501±0.004	1.23
	$T<T_{SI}$	5.794±0.004	–2.5E-4±3E-5	–5.78E-6±1E-7	–0.002±3E-5	0.41	0.499±0.008	
0.535	$T>T_{SI}$	5.781±0.005	7E-4±2E-5	1.45E-6±1E-7	6.5E-4±8E-5	1.45	0.501±0.002	1.28
	$T<T_{SI}$	5.777±0.003	–5.9E-4±1E-5	–2.14E-6±2E-7	–9E-4±4E-5	0.35	0.504±0.008	
0.600	$T>T_{SI}$	5.761±0.001	4.2E-4±2E-5	10.0E-6±2E-7	0.001±5E-5	1.40	0.499±0.006	1.47
	$T<T_{SI}$	5.760±0.007	–4.2E-4±1E-5	–1.90E-6±1E-7	–0.003±8E-5	0.34	0.501±0.001	
0.700	$T>T_{NI}$	5.732±0.001	6.6E-4±1E-5	1.60E-6±1E-7	8.2E-4±2E-5	0.98	0.513±0.004	1.25
	$T<T_{NI}$	5.733±0.002	–0.001±1E-5	20.0E-6±2E-7	–9E-4±4E-5	0.25	0.500±0.002	
0.800	$T>T_{NI}$	5.702±0.001	5.1E-4±1E-5	8.38E-6±1E-7	0.001±2E-5	0.88	0.498±0.002	1.26
	$T<T_{NI}$	5.703±0.036	5.5E-4±1E-5	–2.04E-6±2E-7	–0.001±3E-5	0.23	0.501±0.002	

The similar type of pretransitional behavior for the SmA-I transition is also obtained in some smectogenic cyanobiphenyl liquid crystals [62,66,73]. Therefore, different experimental outcomes confirm that the SmA-I transition is considered to be first order in nature.

Moreover, the absolute value of the ratio (A^N/A^I) is found to lie in the range 1.09 to 2.71 while E_0^N / E_0^I assume values close to unity. These type of values of the critical amplitude ratio are very much equivalent to those reported for other LCs at the N-I [74-75] and SmA-I [62,73] transitions respectively. The fittings lead to a comparable value of the other coefficients as tabulated in Table 6.1. In addition, it has been observed that the critical exponent (α) is nearly equal to 0.5 within the error limit (showing an excellent agreement with the tricritical value) for N-I as well as SmA-I transitions. It certainly confirms that both the transitions are fully compatible with the tricritical behavior and undoubtedly proved the first order character of the aforesaid transitions.

The smectic A to nematic phase transition has also been studied from the density data. In this case the molar volume (V_T) data is not suitable in analyzing the critical behavior at the SmA-N transition due to small change in V_T at T_{SN} compared to the same at T_{NI} or T_{SI}. On the other hand, it has been shown that the thermal expansion coefficient $(-1/\rho)(d\rho/dT)$ is too scattered near the transition (Figure 6.4) and also not appropriate in analyzing the critical behavior. Hence, in analogy with the method adopted earlier in chapter 3 of this thesis (determination of specific heat critical exponent α from Q(T) instead of $-d(\Delta n)/dT$ values) here also a differential quotient R(T) has been considered with the following form:

$$R(T) = -\frac{1}{\rho}\left[\frac{\rho(T) - \rho(T_{SN})}{T - T_{SN}}\right] \tag{6.3}$$

where $\rho(T_{SN})$ is density value at T_{SN}. The parameter R(T) also presents a critical anomaly near T_{SN} with a reasonably smooth variation compared to the thermal expansion coefficient as shown in Figure 6.6. The nature of the SmA-N transition has been assessed by analyzing the limiting behavior of R(T) with the following power law expression (similar to the expression used in chapter 3 for Q(T)) [76]

$$R(T) = A^{\pm}\left|t\right|^{-\alpha} + B^{\pm} \tag{6.4}$$

where A^+ and A^- are the critical amplitudes and B^+ and B^- are the background terms above and below the transition temperature (T_{SN}), α is the critical exponent similar to specific heat capacity critical exponent and $t = |(T - T_{SN})/(T_{SN})|$ is the reduced temperature. Generally, the binary systems containing polar and non polar compounds exhibit Fischer renormalization [77-81] while polar- polar systems are free from it [82]. In addition, Fischer renormalization strongly depends on the slope of smectic A-nematic phase transition line or the steepness of phase boundary. Applicability of Fischer renormalization has been verified for this binary system (7CB+ME6O.5) by determining a suitable parameter to characterize this dependence *i.e.* the slope of $\ln T_{SN}$ *vs.* concentration curve. For the SmA-N phase boundary of 7CB+ME6O.5 the slope $[d(\ln T_{SN})/dx)]^2$ assumes values between 0.060 to 0.207 which is less compared to the same reported by others for polar-non polar binary systems showing Fischer renormalization [79-81].

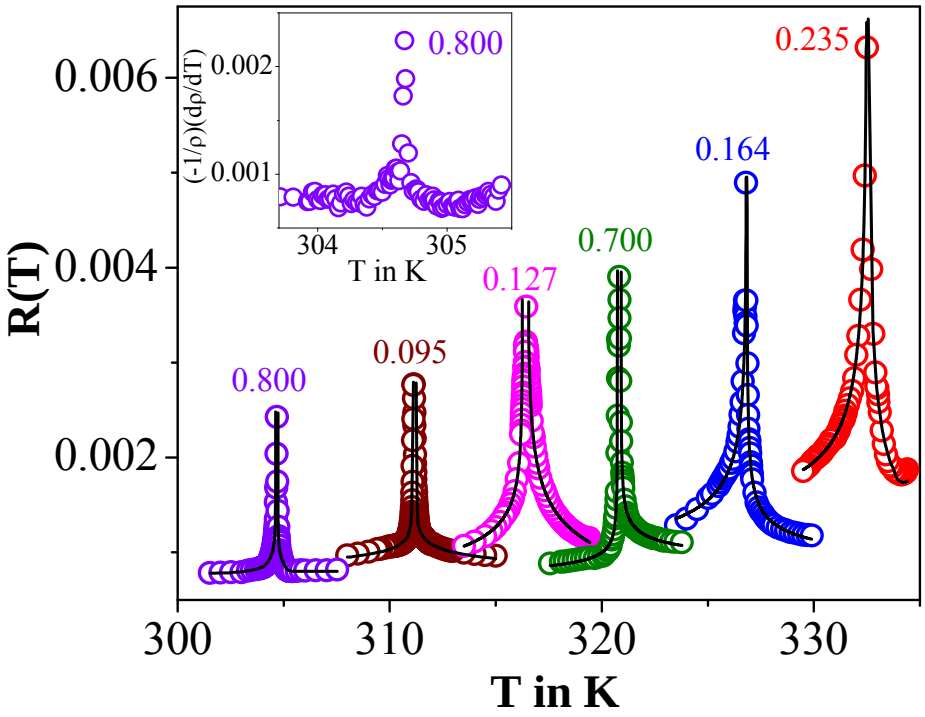

Figure 6.6 R(T) as a function of temperature for some mixtures in the vicinity of SmA-N transition. Solid lines represent the fit according to Equation (6.4). For better representation R(T) data for the following three concentrations x_{7CB} = 0.095, 0.127 and 0.700 has been shifted by –8K, –5K and +3K respectively. In the inset variation of thermal expansion coefficient for x_{7CB} = 0.800 is illustrated.

If $[d(\ln T_{SN})/dx)]^2$ lies between 0.74 to 9.0 or more then Fischer renormalization is expected to occur [79-80]. The SmA-N transitions for the present binary system are free from Fischer renormalization due to comparatively small value of $[d(\ln T_{SN})/dx)]^2$. The positive α values describing the critical behavior at the SmA-N transition lies in the range 0.036 to 0.512 within the limit of uncertainty as listed in Table 6.2. Now the consistency of α values as obtained from the fit to R(T) data has been checked with the same obtained from high resolution birefringence (Δn) data. Figure 6.7(a) depicts temperature dependence of birefringence for three representative concentrations of 7CB. Following the similar procedure as adopted earlier (in Chapter 3) the specific heat critical exponent (α) has been determined from the transitional divergence of Q(T) which has been derived from birefringence. Figure 6.7(b) illustrates Q(T) data near the SmA-N transition.

Table 6.2 The best fit parameter values for R(T) near the SmA-N transition of the binary system 7CB+ME6O.5 obtained from Equation (6.4).

x_{7CB}		A^- or A^+	α	B^- or B^+	χ^2	No of data points
0.095	$T<T_{SN}$	0.0008±0.00001	0.067±0.007	-0.0002±0.00001	1.45	80
	$T>T_{SN}$	0.0009±0.00002	0.068±0.002	-0.0003±0.00001	1.51	82
0.127	$T<T_{SN}$	0.0008±0.00004	0.153±0.004	-0.0005±0.00006	1.68	51
	$T>T_{SN}$	0.0013±0.00003	0.143±0.003	-0.0015±0.00003	1.59	38
0.164	$T<T_{SN}$	0.0002±0.00001	0.332±0.028	0.0005±0.00002	1.55	27
	$T>T_{SN}$	0.0001±0.00001	0.345±0.013	0.0007±0.00003	1.49	34
0.235	$T<T_{SN}$	0.0001±0.00002	0.512±0.004	0.0010±0.00002	1.66	24
	$T>T_{SN}$	0.0001± 0.00001	0.509±0.008	0.0010±0.00001	1.69	39
0.700	$T<T_{SN}$	0.0001±0.00002	0.314±0.045	0.00062±0.00002	1.59	32
	$T>T_{SN}$	0.0001±0.00004	0.309±0.008	0.00074±0.00003	1.41	42
0.800	$T<T_{SN}$	0.0023±0.00001	0.039±0.014	-0.0021±0.00001	1.75	51
	$T>T_{SN}$	0.0025±0.00003	0.036±0.016	-0.0023±0.00001	1.61	51

From the fitting of both R(T) and Q(T) data it has been observed that the SmA-N transition exhibits a crossover from second order to first order nature with α varying from 0.036 to 0.512 within the error limit. All the studied mixtures shows second order SmA-N transition except $x_{7CB} = 0.235$ for which the critical exponent is found to be ~ 0.5 indicating a first order nature of SmA-N transition.

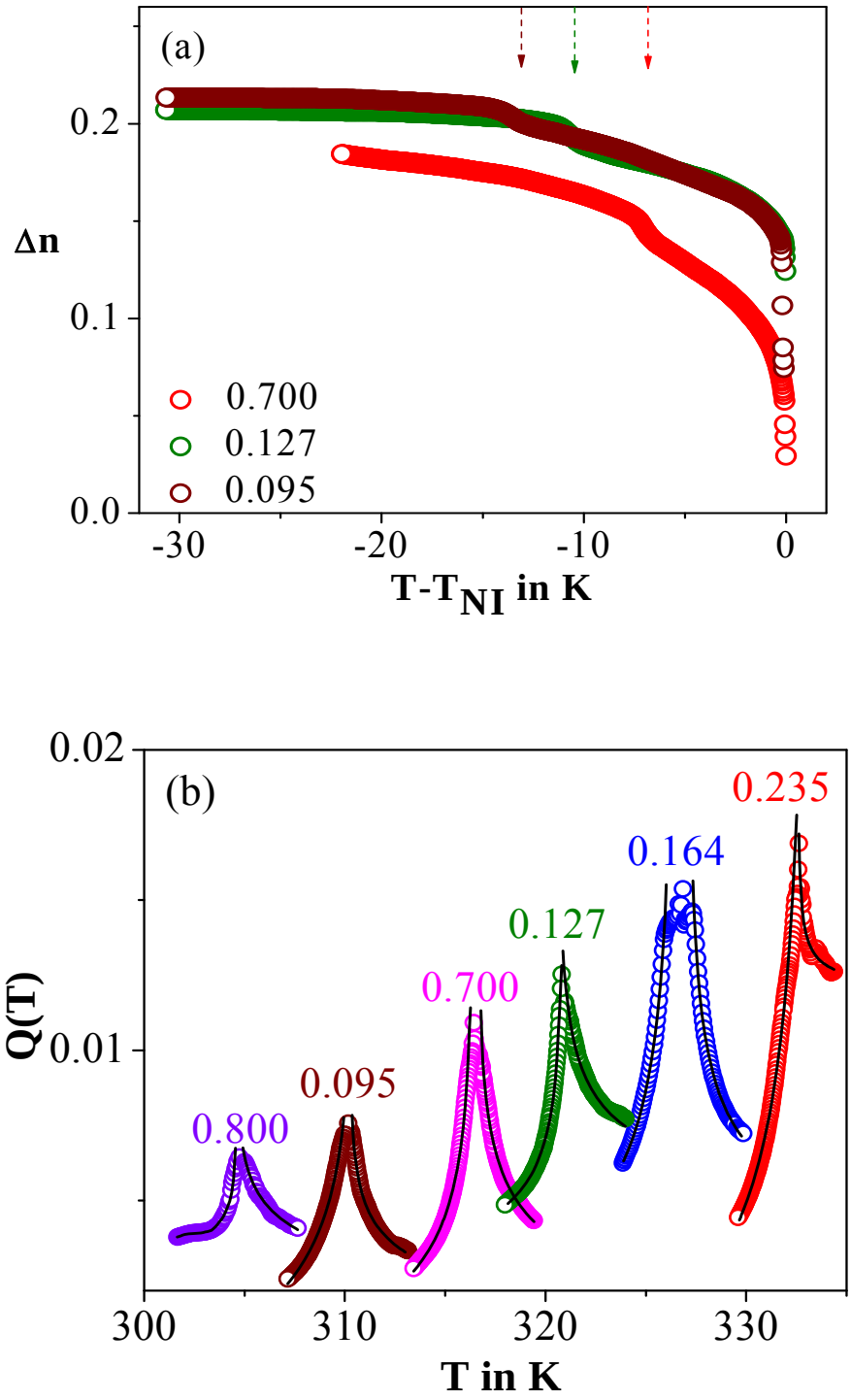

Figure 6.7(a) Birefringence as a function of temperature for three concentrations. Dashed lower head arrow denotes T_{SN}. **(b)** Q(T) as a function of temperature near SmA-N transition. Solid lines represent the fit according to Equation (3.4). For better representation Q(T) data for the following three concentrations x_{7CB} = 0.095, 0.127 and 0.700 has been shifted by –8K, –5K and +3K respectively.

Table 6.3 The best fit parameter values for Q(T) near the SmA-N transition of the binary system 7CB+ME6O.5 obtained from Equation (3.4).

x_{7CB}		A^- or A^+	α	B^- or B^+	χ^2	No of data points
0.095	$T<T_{SN}$	0.0202±0.0001	0.088±0.007	-0.0280±0.00011	1.55	108
	$T>T_{SN}$	0.0100±0.0001	0.087±0.002	-0.0103±0.0009	1.68	112
0.127	$T<T_{SN}$	0.0050±0.0003	0.153±0.004	-0.0100±0.0002	1.48	114
	$T>T_{SN}$	0.0044±0.0002	0.143±0.003	-0.0061±0.0001	1.47	109
0.164	$T<T_{SN}$	0.0020±0.00001	0.344±0.028	-0.0046±0.0002	1.52	45
	$T>T_{SN}$	0.0014±0.00001	0.345±0.013	-0.0042±0.0001	1.68	50
0.235	$T<T_{SN}$	0.0012±0.0002	0.505±0.002	-0.0070±0.00002	1.45	113
	$T>T_{SN}$	0.0010±0.0001	0.501±0.004	0.0116±0.00001	1.48	71
0.700	$T<T_{SN}$	0.0010±0.0001	0.334±0.045	0.0021±0.0001	1.39	113
	$T>T_{SN}$	0.0011±0.0001	0.331±0.008	0.0025±0.0001	1.57	123
0.800	$T<T_{SN}$	0.0131±0.0007	0.043±0.001	-0.0126±0.0006	1.61	63
	$T>T_{SN}$	0.0205±0.0009	0.045±0.001	-0.0212±0.0007	1.49	57

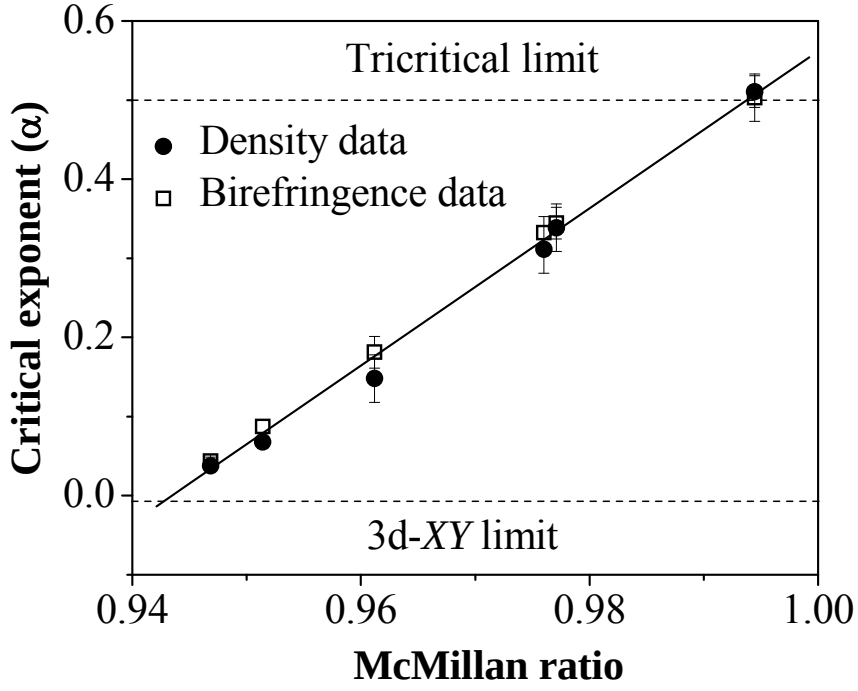

Figure 6.8 Variation of critical exponent with McMillan ratio for some concentrations of the binary system 7CB+ME6O.5 obtained from two sets of measurements *i.e.* density and birefringence data. (● or □) represents the α values averaged over the two values obtained from fitting above and below the transition temperature T_{SN}. Solid line represents a polynomial fit to the α values.

The two sets of α values (listed in Table 6.2 and 6.3) has been plotted against the McMillan ratio in Figure 6.8 which clearly demonstrates that both the high resolution density as well as birefringence measurements yields comparable α values at the SmA-N transition. Moreover, a polynomial fit to the extracted α results a particular value of McMillan ratio 0.994 for which critical exponent attains the tricritical value 0.5. Interestingly, this polar-non polar induced smectic-A binary system (7CB+ME6O.5) have two tricritical points (TCP) on either sides of the phase diagram at x_{7CB} = 0.232 and 0.627 respectively (shown by the arrow mark in Figure 6.1).

6.5 Conclusion

A precise high resolution method with reasonably good accuracy (±0.00005 g/cm^3) has been carried out to measure the temperature variation of density of some binary mixtures exhibiting induced smectic A phase. The density data shows a clear evidence of pretransitional behavior in the vicinity of N-I or SmA-I phase transition due to the enhancement of the molecular ordering. The appearance of pretransitional anomaly has been observed for both the N-I and SmA-I transitions and analysis have been carried out to obtain the values of discontinuity, the hypothetical continuous phase transition temperatures and the metastable region to probe the critical behavior at the phase transitions. Particular emphasis has been devoted to determine the spinodal temperatures T* and T** from the very precise changes of molar volume in the vicinity of the N-I and SmA-I transitions. The discontinuity (ΔT*) at the clearing temperature is one of the basic characteristics of the N-I or SmA-I transitions which is amounted to several degrees and is found to be substantially higher for SmA-I transition than the N-I transition. The consistent values of T_{NI}-T* or T**-T_{NI} favors that the N-I and SmA-I transitions are fully compatible with the tricritical nature. It should be stressed that the width of the metastable region for the N-I transition is less than that found for the SmA-I transition. This fact can easily be extracted from the comparison of density change for both phase transitions.

Moreover, by exploiting the fact that the thermal expansion coefficient near the clearing temperature exhibit the same power law divergence as the specific

heat capacity, the effective critical exponent α has been extracted by a fit to the $\ln V_T$ data which is directly linked to the thermal expansion coefficient. The critical exponent α for the N-I and SmA-I transitions has been found to reach the tricritical value 0.5 within the error limit. Also it indicates the fluid like resemblance in the isotropic phase of the SmA-I phase transition. Therefore, this high resolution density measurement can be successfully applied to study the pretransitional effects near the phase transitions as well as the nature of the phase transitions in liquid crystal systems.

Additionally, the SmA-N transition has also been reviewed from the high resolution density data which is very much useful in determining the order character of the same. Nevertheless the outcomes of density measurements have also been compared with high resolution birefringence measurements and these two sets of data show a very good agreement. Finally, this induced binary system endows with two tricritical points (TCP) located at $x_{7CB} = 0.232$ and 0.627 on both sides of phase diagram at which the SmA-N transition changes its character from second order to first order.

References

[1] E. Gulari, B. Chu, Density of methoxybenzylidene butylaniline about the isotropic–nematic phase transition, *J. Chem. Phys.*, **62**, 795 (1975).

[2] S. Torza, P.E. Cladis, Volumetric Study of the Nematic-Smectic-A Transition of N− p− Cyanobenzylidene− p− Octyloxyaniline, *Phys. Rev. Lett.*, **32**, 1406 (1974).

[3] B. Bahadur, Specific volume studies on some nematic liquid crystals, *Z. Naturforsch.*, **30a**, 1094 (1975).

[4] W. Maier, A. Saupe, Eine einfache molekular-statistische theorie der nematischen kristallinflüssigen phase. Teil II, *Z. Naturforsch.*, **15a,** 287 (1960).

[5] M.J. Press, A.S. Arrott, Expansion coefficient of methoxybenzylidene butylaniline through the liquid-crystal phase transition, *Phys. Rev. A*, **8**, 1459 (1973).

[6] D. Armitage, F.P. Price, Volumetric behavior of liquid crystal Np-cyanobenzylidene-p-octyloxyaniline, *Mol. Cryst. Liq. Cryst.*, **38**, 229, (1977).

[7] I. Zgura, R. Moldovan, T. Beica, S. Frunza, Temperature dependence of the density of some liquid crystals in the alkyl cyanobiphenyl series, *Cryst. Res. Technol.*, **44(8)**, 883 (2009).

[8] D. Demus, J. Goodbye, G.W. Gray, H.-W. Spiess (eds.), Handbook of liquid crystals, Vol 1, V. Vill, Wiley-VCI, Weinheim, New York, Chiche, Brisbane, Singapore, Toronto (1998).

[9] D. Armitage, F.P. Price, Volumetric study of the nematic-isotropic pretransition region, *Phys. Rev. A*, **15**, 2496 (1977).

[10] A.J. Leadbetter, J.L.A. Durant, M. Rugman, The density of 4 n-octyl-4-cyano-biphenyl (8CB), *Mol. Cryst. Liq. Cryst. Lett.*, **34**, 231 (1977).

[11] D.A. Dunmur, W.H. Miller, Volumetric studies of the homologous series of alkyl-cyano-biphenyl liquid crystals, *J. Phys. Coll. (Paris)*, **40**, C3-141 (1979).

[12] H.R. Zeller, Dielectric relaxation in nematics and Doolittle's law, *Phys. Rev. A*, **26**, 1785 (1982).

[13] T. Beica, R. Moldovan, I. Zgura, S. Frunza, Interfacial tension of some liquid crystals in the cyanobiphenyl series at the interface with glycerol, *J. Opt. Adv. Mater.*, **11**, 3624 (2007).

[14] J. Deschamps, J.P.M. Trusler, G. Jackson, Vapor pressure and density of thermotropic liquid crystals: MBBA, 5CB, and novel fluorinated mesogens, *J. Phys. Chem. B*, **112**, 3918 (2008).

[15] G.A. Oweimreen, The effect of quasispherical solutes on the smectic-a− nematic and nematic− isotropic phase equilibria in pn-alkyl-p'-cyanobiphenyl liquid crystals, *J. Phys. Chem. B*, **105**, 8410 (2001).

[16] M.K. Das, R. Paul, Optical birefringence, density and order parameter of an ester-biphenyl mixture exhibiting an injected smectic phase, *Phase Transit.*, **46**, 185 (1994).

[17] A. Zywocinski, S.A. Wieczorek, J. Stecki, High-resolution volumetric study of the smectic-A -to-nematic transition in 4-(n-pentyl)phenylthiol-4'-(n-octyloxy)benzoate (SSS) and octyloxycyanobiphenyl (8OCB), *Phys. Rev. A*, **36**, 190 (1987).

[18] J. Lalitha Kumari, P.V. Datta Prasad, M.R.N. Rao, D. Madhavilatha, V.G.K.M. Pisipati, Synthesis, characterization and phase transition studies across different liquid crystalline phases in nO.O4 compounds, *Phase Transit.*, **84(7)**, 639 (2011).

[19] A. Zywocinski, Spinodal temperatures at the nematic to isotropic phase transition from precise volumetric measurements, *J. Phys. Chem. B*, **107,** 9491 (2003).

[20] J. Salud, P. Cusmin, M.R. de la Fuente, M.A. Perez-Jubindo, D.O. Lopez, S. Diez-Berart, Study of the critical behavior and scaling relationships at the N-to-I phase transition in hexyloxycyanobiphenyl, *J. Phys. Chem. B*, **113**, 15967 (2009).

[21] P. Cusmin, M.R. de la Fuente, J. Salud, M.A. Pe´rez-Jubindo, S. Diez-Berart, D.O. Lo´pez, Critical behavior and scaling relationships at the smad-n and n-i transitions in nonyloxycyanobiphenyl (9OCB), *J. Phys. Chem. B*, **111,** 8974 (2007).

[22] P. Cusmin, J. Salud, D.O. Lopez, S. Diez-Berart, M.R. de la Fuente, M.A. Pe´rez-Jubindo, N. Veglio, Overall analysis of first-order phase transitions

in some alkyloxycyanobiphenyl liquid crystals, *Liq. Cryst.*, **35(6)**, 695 (2008).

[23] W.H. de Jeu, L. Longa, D. Demus, Simple model of induced smectic phases in binary mixtures of liquid crystals, *J. Chem. Phys.*, **84**, 6410 (1986).

[24] L.K.M. Chen, G.W. Gray, D. Lacey, S. Srilhauratana, K.L. Toyne, Reentrant nematic and injected smectic behaviour in binary mixtures including those of terminally non-polar compounds, *Mol. Cryst. Liq. Cryst.*, **150**, 335 (1987).

[25] K. Araya, Y. Matsunaga, Liquid crystal formation in binary systems. II. Induction of nematic and smectic phases by electron donor-acceptor interaction between the *p*-dimethylamino and *p*-nitro derivatives of *n*-benzylideneaniline, *Bull. Chem. Soc. Jap.*, **53**, 3079 (1980).

[26] N.K. Sharma, G. Pelzl, D. Demus, W. Weissflog, EDA complexes from 2 liquid-crystal components, *Z. Phys. Chem.*, **261**, 579 (1980).

[27] M.K. Das, R. Paul, D.A. Dunmur, Small angle x-ray diffraction studies of an ester/biphenyl mixture (5CB/ME 50.5) showing an injected smectic phase, *Mol. Cryst. Liq. Cryst.*, **258**, 239 (1995).

[28] S. Garg, T. Spears, Dielectric properties of a nematic binary mixture, *Mol. Cryst. Liq. Cryst.*, **409**, 335 (2004).

[29] P.D. Roy, S. Paul, M.K. Das, Dielectric permittivity studies of nematogenic compounds and their binary mixtures showing induced smectic A_d phase, *Phase Transit.*, **79**, 323 (2006).

[30] P.D. Roy, A. Prasad, M.K. Das, Study of the physical properties of a mesogenic mixture showing induced smectic A_d phase by refractive index, density and x-ray diffraction measurements, *J. Phys.: Condens. Matter*, **21**, 075106 (2009).

[31] P.G. de Gennes, J. Prost, The physics of liquid crystals, Clarendon Press, Oxford (1993).

[32] S. Chandrasekhar, Liquid Crystals, Cambridge University press, Cambridge (1992).

[33] P.K. Mukherjee, The T_{NI} –T* puzzle of the nematic–isotropic phase transition, *J. Phys.: Condens. Matter*, **10**, 9191 (1998).

[34] M.A. Anisimov, Critical phenomena in liquids and liquid crystals, Gordon and Breach, Philadelphia (1991).

[35] E.F. Gramsbergen, L. Longa W.H. de Jeu, Landau theory of the nematic-isotropic phase transition, *Phys. Rep.*, **135**, 195 (1986)

[36] S. Singh, Phase transitions in liquid crystals, *Phys. Rep.*, **324**, 107 (2000).

[37] P.K. Mukherjee, T.R. Bose, D. Ghose, M. Saha, Inclusion of density variation in the Landau–de Gennes theory of the nematic-isotropic phase transition, *Phys. Rev. E*, **51**, 4570 (1995).

[38] A. Drozd-Rzoska, S.J. Rzoska, J. Zioło, Critical behavior of dielectric permittivity in the isotropic phase of nematogens, *Phys. Rev. E*, **54(6)**, 6452 (1996).

[39] S. Yildiz, H. Ozbek, C. Glorieux, J. Thoen, Critical behaviour at the isotropic–nematic and nematic–smectic A phase transitions of 4-butyloxyphenyl 4'-decyloxybenzoate liquid crystal from refractive index data. *Liq. Cryst.*, **34(5)**, 611 (2007).

[40] M.A. Anisimov, S.R. Garber, V.S. Esipov, V.M. Mamnitskii, G.I. Ovodov, L.A. Smolenko, E.L. Sorkin, Anomaly of the specific heat and the nature of the phase transition from an isotropic liquid to a nematic liquid crystal, *Sov. Phys. JETP.*, **45**, 1042 (1977).

[41] P.K. Mukherjee, Isotropic to smectic-A phase transition: A review, *J. Mol. Liq.*, **190**, 99 (2014).

[42] F.V. Chavez, R.H. Acosta, D.J. Pusil, Molecular dynamics above the smectic A-isotropic phase transition of thermotropic liquid crystals studied by NMR, *Chem. Phys. Lett.*, **392**, 403 (2004).

[43] S.G. Polushin, V.B. Rogozhin, E.I. Ryumtsev, A.V. Lezov, The Kerr effect in the vicinity of the transition from the isotropic to smectic a phase, *Russ. J. Phys. Chem.*, **80**, 1016 (2006).

[44] G. Cordoyiannis, L.F.V. Pinto, M.H. Godinho, C. Glorieux, J. Thoen, High-resolution calorimetric study of the phase transitions of tridecylcyanobiphenyl and tetradecylcyanobiphenyl liquid crystals, *Phase Transit.*, **82**, 280 (2009).

[45] D. Demus, L. Richter, Textures of liquid crystals, Verlag Chemie, Weinheim (1978).

[46] I. Dierking, Textures of liquid crystals, Wiley-VCH, Weinheim (2003).

[47] B.R. Rajeswari, P. Pardhasaradhi, M.R.N. Rao, P.V. Datta Prasad, D. Madhavi Latha, V.G.K.M. Pisipati, Phase transition studies in (p-n-phenylbenzylidene)-p-alkoxy anilines, *J. Therm. Anal. Calorim.*, **111**, 561 (2013).

[48] P.V. Datta Prasad, M.R.N. Rao, V.G.K.M. Pisipati, Phase transition studies in liquid crystals across i-n and n-sc phases in alkoxy benzoic acids – density measurements, *Mol. Cryst. Liq. Cryst.*, **511**, 112/[1582] (2009).

[49] A.A. Barbosa, A.J. Palangana, Comparison between densitometer and dilatometer measurements in liquid-crystal phases, *Phys. Rev. E*, **56(2)**, 2295 (1997).

[50] K. Fakruddin, R. Jeevan Kumar, V.G.K.M. Pisipati, D. Madhavi Latha, B.T.P. Madhav, P.V. Datta Prasad, Phase transitions and thermodynamic parameters of n-(p-n-octyloxybenzylidene)-p-nalkoxyanilines— a dilatometric study, *Mol. Cryst. Liq. Cryst.*, **524**, 102 (2010).

[51] E. Anesta, G.S. Iannacchione, C.W. Garland, Critical linear thermal expansion in the smectic-A phase near the nematic-smectic phase transition, *Phys. Rev. E*, **70**, 041703 (2004).

[52] A. Zywociński, SA Wieczorek, High-resolution volumetric study of the smectic-A-smectic-C transition in 4-(n-pentyl)phenylthio-4'-(n-octyl)oxybenzoate (8S5), *Phys. Rev. A*, **31**, 479 (1985).

[53] A.B. Pippard, Thermodynamic relations applicable near a lambda-transition, *Philos. Mag.*, **1**, 473 (1956).

[54] C.W. Garland, Generalized Pippard equations, *J. Chem. Phys.*, , **41**, 1005 (1964).

[55] P.H. Keyes, Tricritical behavior at the isotropic-nematic transition, *Phys. Lett. A*, **67**, 132 (1978).

[56] P.R. Bevington, Data reduction and error analysis for the Physical Sciences, McGraw Hill, New York (1969).

[57] M.A. Anisimov, Universality of the critical dynamics and the nature of the nematic-isotropic phase transition, *Mol. Cryst. Liq. Cryst.*, **146**, 435 (1987).

[58] C. Rosenblatt, Evidence for classical critical behavior at the nematic-isotropic phase transition, *Phys. Rev. A*, **27**, 1234 (1983**)**.

[59] A.J. Nicastro, P.H. Keyes, Electric-field-induced critical phenomena at the nematic-isotropic transition and the nematic-isotropic critical point, *Phys. Rev. A*, **30**, 3156 (1984).

[60] P.V. Kolinsky, B.R. Jennings, Optical Kerr effect in the isotropic phase of various alkyl-cyanobiphenyl homologues, *Mol. Phys.*, **40**, 979 (1980**)**.

[61] G. Czechowski, J. Jadzyn, J. Zioło, S.J. Rzoska, M. Paluch, Linear and non-linear dielectric pretransitional behavior near the isotropic-nematic phase transition for 4-cyano-4-n-pentylbiphenyl (5CB), *Z. Naturforsch. A*, **46**, 244 (2002**)**.

[62] A. Drozd-Rzoska, S. J. Rzoska, K. Czupryn´ski, Phase transitions from the isotropic liquid to liquid crystalline mesophases studied by linear and nonlinear static dielectric permittivity, *Phys. Re*v. *E*, **61**, 5355 (2000).

[63] S.J. Rzoska, J. Zioło, W. Sułkowski, J. Jadzùyn, G. Czechowski, Fluidlike behavior of dielectric permittivity in a wide range of temperature above and below the nematic-isotropic transition, *Phys. Rev. E*, **64**, 052701 (2001).

[64] A. Drozd-Rzoska, Quasicritical behavior of dielectric permittivity in the isotropic phase of n-hexyl-cyanobiphenyl in a large range of temperatures and pressures, *Phys. Re*v. *E*, **59**, 5556 (1999).

[65] J. Thoen, G. Menu, Temperature dependence of the static relative permittivity of octylcyanobiphenyl (8CB), *Mol. Cryst. Liq. Cryst.*, **97**, 163 (1983).

[66] A. Drozd-Rzoska, S.J. Rzoska, J. Zioło, Quasicritical behavior of dielectric permittivity in the isotropic phase of smectogenic n-cyanobiphenyls, *Phys. Rev. E*, **61**, 5349 (2000).

[67] S.K. Sarkar, M.K. Das, Critical behavior of dielectric permittivity in the vicinity of nematic–isotropic and smectic–nematic phase transitions in smectogenic binary mixtures, *Fluid Phase Equilib*., **365**, 41 (2014).

[68] S.K. Sarkar, M.K. Das, Dielectric studies and critical behaviour in the vicinity of nematic–isotropic phase transition of a smectogenic binary mixture showing induced nematic phase, *Liq. Cryst.*, **41**, 1410 (2014).

[69] S.K. Sarkar, P.C. Barman, M.K. Das, Optical birefringence and its critical behavior in the vicinity of nematic–smectic A phase transition in a binary mixture, *Physica B*, **446**, 80 (2014).

[70] S.K. Sarkar, M.K. Das, Order parameter and its critical exponent for some binary mixtures showing induced nematic phase, *Phase Transit.*, **89(9)**, 910 (2016).

[71] B.M. Ocko, A. Braslau, P.S. Pershan, J. Als-Nielsen, M. Deutsch, Quantized layer growth at liquid-crystal surfaces, *Phys. Rev. Lett.*, **57**, 94 (1986).

[72] M. Olbrich, H.R. Brand, H. Finkelmann, K. Kawasaki, Fluctuations above the smectic-A-isotropic transition in liquid crystalline elastomers under external stress, *Europhys. Lett.*, **31**, 281 (1995).

[73] A. Drozd-Rzoska, Influence of measurement frequency on the pretransitional behaviour of the no-linear dielectric effect in the isotropic phase of liquid crystalline materials, *Liq. Cryst.*, **24**, 835 (1998).

[74] S. Diez, D.O. Lopez, M.R. De la Fuente, M.A. Perez-Jubindo, J. Salud, J. Ll. Tamarit, Thermodynamic and dielectric studies concerning the influence of cylindrical submicrometer confinement on heptyloxycyanobiphenyl, *J. Phys. Chem. B*, **109**, 23209 (2005).

[75] G.S. Iannacchione, D. Finotello, Specific heat dependence on orientational order at cylindrically confined liquid crystal phase transitions, *Phys. Re*v. *E*, **50**, 4780 (1994).

[76] S. Erkan, M. Cetinkaya, S. Yildiz, H. Ozbek, Critical behavior of a nonpolar smectoge from high-resolution birefringence measurements, *Phys. Rev. E*, **86**, 041705(1) (2012).

[77] M.E. Fisher, Renormalization of critical exponents by hidden variables, *Phys. Rev.*176, 257 (1968).

[78] M.E. Fisher, P.E. Scesney, Renormalization of critical exponents by hidden variables, *Phys. Rev.A*, 2, 825 (1970).

[79] M.E. Huster, K.J. Stine, C.W. Garland, Calorimetric study of nematic-smectic-A tricritical behavior in mixtures of heptyloxypentylphenylthiolbenzoate and octyloxycyanobiphenyl, *Phys. Rev. A*, **36**, 2364 (1987).

[80] K.J. Stine, C.W. Garland, Calorimetric study of Fisher renormalization of tricritical behavior in mixtures of octyloxycyanobiphenyl and terephtal-bis-butylaniline, *Phys. Rev. A*, **39**, 1482 (1988).

[81] J. Caerels, C. Glorieux, J. Thoen, Photopyroelectric ac calorimetric study of the nematic–smectic-A phase-transition line in binary liquid crystal mixtures with injected smectic-A phases, *Phys. Rev. E*, **65**, 031704 (2002).

[82] M.B. Sied, J. Salud, D.O. Lopez, M.Barrio, J.Ll. Tamarit, Binary mixtures of nCB and nOCB liquid crystals. Two experimental evidences for a smectic A–nematic tricritical point, *Phys. Chem. Chem. Phys.*, **4**, 2587 (2002).